



FACULTY OF SCIENCE AND TECHNOLOGY

## MASTER THESIS

Study programme / specialisation:

LFYMAS-1  
Masteroppgave fysikk - Lektor

The spring semester, 2022

Author:  
Liva Sandvin Vangen

Open

*Liva S. Vangen*  
(signature author)

Course coordinator: Alex Nielsen

Supervisor(s): Helena Kolesova

Thesis title:  
The dark matter freeze out and beyond

Credits (ECTS): 30

Keywords:  
- Dark matter  
- Thermal freeze out  
- DarkSUSY  
- WIMP  
- Scalar singlet  
- Detection experiments of DM  
- Freeze in

Pages: .....62.....  
+ appendix: .....5.....

Stavanger, ...15/06/2022.....  
date/year

---

Approved by the Dean 30 Sep 21  
Faculty of Science and Technology

# The dark matter freeze out and beyond

Liva Sandvin Vangen

Spring 2022

## Abstract

Evidence of the existence of dark matter has been found due to deviations of gravitational motion of astronomical objects. We want to investigate the dark matter topic, which is constantly evolving due to the fast development of technology today. The thermal freeze out of dark matter has been proposed to be the production mechanism of DM in the Universe. We look into this production mechanism, and the properties of dark matter that follows from it. We derive the Boltzmann equation of the thermal freeze out approximately analytical, to study the thermodynamic properties of the freeze out. By the use of the Fortran-program DarkSUSY, a calculation program for DM properties, we calculate precise values of the same properties. By comparing observational values of dark matter with our derivations and calculations, we can learn about the non-gravitational properties of DM. We further introduce some dark matter particle candidates, the generic weakly interacting massive particle (WIMP), and the scalar singlet.

The freeze out production mechanism has not been confirmed, because the particle candidates have not been detected. Due to this, we look further into alternative production mechanisms. The freeze in production mechanism of dark matter has been proposed, with the corresponding dark matter particle candidate FIMP (feebly interacting massive particle), and we look briefly into this.

## Acknowledgements

I would like to give thanks to my supervisor Helena Kolesova, postdoctor at the Department of Mathematics and Physics at the University of Stavanger. Thank you for your guidance with the thesis throughout the semester, and for always keeping a good spirit.

I would also like to thank fellow student Stine Aunøyen Norli, who wrote a bachelor thesis of the same topic simultaneously. Thank you for instructive discussions of the topic, and good collaboration with the program DarkSUSY. Thank you to the library at the University of Stavanger for providing me with the necessary books and articles to complete the thesis, and for guidance with references.

Lastly, I would like to thank all my friends and family who supported me throughout this semester, and especially thanks to Jørgen Holth.

# Contents

<b>1</b>	<b>Introduction</b>	<b>7</b>
<b>2</b>	<b>Background theory</b>	<b>9</b>
2.1	Cosmology . . . . .	9
2.2	Particle physics . . . . .	12
2.2.1	The Standard Model . . . . .	12
2.2.2	Higgs mechanism . . . . .	13
2.2.3	Beyond the Standard Model . . . . .	14
2.3	Statistical physics . . . . .	15
2.4	DarkSUSY . . . . .	17
<b>3</b>	<b>Evidence for dark matter</b>	<b>18</b>
3.1	Early history . . . . .	18
3.2	Observational evidence . . . . .	19
3.3	Nature of dark matter . . . . .	22
<b>4</b>	<b>Thermal freeze out of dark matter</b>	<b>25</b>
4.1	Boltzmann equation . . . . .	25
4.2	Applications of the Boltzmann equation . . . . .	27
4.3	Relic abundance in case of thermal freeze out . . . . .	30
4.4	DarkSUSY results . . . . .	32
4.4.1	The generic WIMP module . . . . .	32
4.4.2	Calculations of relic abundance . . . . .	33
4.4.3	Calculations of average annihilation cross section . . . . .	35
4.4.4	Calculations of freeze out $x$ . . . . .	37
4.4.5	Calculations of the yield . . . . .	41
4.5	The WIMP miracle . . . . .	42
<b>5</b>	<b>Scalar singlet</b>	<b>44</b>
5.1	DarkSUSY results . . . . .	46
5.1.1	Silveira-Zee module . . . . .	46
5.1.2	Calculations of relic abundance . . . . .	46
<b>6</b>	<b>Experimental detection of dark matter</b>	<b>49</b>
6.1	Indirect detection . . . . .	49
6.2	Collider searches . . . . .	50
6.3	Direct detection . . . . .	51
6.3.1	Constraints of dark matter . . . . .	51
6.3.2	Constraints of scalar singlet dark matter . . . . .	52

<b>7</b>	<b>Freeze in of scalar singlet DM</b>	<b>55</b>
7.1	DarkSUSY results . . . . .	57
<b>8</b>	<b>Conclusion</b>	<b>58</b>
<b>A</b>	<b>List of abbreviations</b>	<b>63</b>
<b>B</b>	<b>Programming in DarkSUSY</b>	<b>64</b>

# 1 Introduction

Almost 85% of the total mass in the Universe is made up of a mysterious type of matter, called dark matter (DM) [1]. This matter, and its nature, is one of the most intriguing questions of both cosmology and particle physics today. Dark matter does not reflect or emit light, and even though this prevents us to observe the dark matter directly, there has been observed gravitational evidence of the existence of DM [1].

By the study of deviating gravitational motion of astronomical objects many years ago, the suspicion of an invisible form of matter grew [2]. In the 1930s, physicist Fritz Zwicky was the first to propose the model of DM we know today [2]. It took a while before other physicists accepted the DM theory, but in the recent decades the knowledge and evidence of DM has increased significantly. Theories of DM production and DM particle candidates have emerged, and new observations of the nature of DM has been made.

Even though we have significant evidence of the existence of dark matter in the Universe, we do not know a lot about the nature of this type of matter. By the observation of a bullet cluster in 2006 [3], it was discovered that the nature of dark matter was different than for baryonic matter. The dark matter was observed to barely be self-interacting, and barely interacting with baryonic matter. As this is different from baryonic matter, this indicated that dark matter is non-baryonic matter.

Many dark matter particle candidates have been proposed through the years, and one of the most studied models is the weakly interacting massive particle (WIMP) model [4]. As the standard model (SM) do not provide us with such a particle, this is a yet undiscovered particle. To predict the existence of this particle we need to consider extensions of the SM, such as supersymmetric particles or the addition of a real singlet scalar field.

DM is a widely studied field in both cosmology and particle physics today. Even though the technology to study the nature of DM is quickly evolving, there is still a lot of unanswered questions of the topic. Our knowledge of DM evolves in line with the technology, and one will therefore most likely make new observations of the topic of DMs nature in the coming decades. This is why this topic is highly relevant to investigate as of today.

By our knowledge of the early Universe and cosmology, we want to look into if we can learn about the non-gravitational properties of dark matter. We will in this thesis investigate some proposed models for the production mechanism of dark matter, and the corresponding properties of DM based on this. Production models of DM explains the DM production with correct properties from

the early Universe, and correct amount of DM today. The production model we will focus on, the most thoroughly studied model, is called the *thermal freeze out* of dark matter. This is a popular production model of DM, because it predicts the existence of a WIMP, a particle that is in accordance with supersymmetric dark matter and other models. In addition, we will briefly look into an alternative model of production mechanism, *the freeze in* of dark matter.

In this thesis we will firstly look into some necessary background theory of particle physics and cosmology, in section 2. This is necessary to get an understanding of the models of the dark matter production. Next, in section 3, we will look at evidence for dark matter, and some observations that have determined what we already know about the nature of dark matter. In the next section, section 4, we will investigate thermodynamic properties of the thermal freeze out of dark matter. We will derive some formulas to explain what happens in this process, and find some values for the average annihilation cross section and relic abundance of DM in this case. In section 4.4 we consider specific examples of properties of dark matter in the case of thermal freeze out. We do this by the use of the DM calculation program DarkSUSY [5]. This program calculates properties of dark matter, by the choice of specific DM particle characteristics. We introduce a specific WIMP model, scalar singlet, in section 5. In this section we investigate the properties of the scalar singlet model for the dark matter particles, and how this fits with our previous calculations and derived formulas. Next, in section 6, we will explain some probable detection experiments, that should be able to detect dark matter if our freeze out model is correct. We will look at both indirect and direct detection, in addition to collider searches. Lastly, we will briefly look into a new production model, the freeze in, in section 7, before we end the thesis with a conclusion in section 8. We include a list of abbreviations in Appendix A, and some details of the programming in DarkSUSY in Appendix B.



## 2 Background theory

In this section we will briefly look into some standard knowledge of cosmology, particle physics and statistical physics. This is knowledge required to get an understanding of the theory later in this thesis. When describing cosmological scenarios, we use natural units, where  $c = \hbar = k_B = 1$ . We will use these units throughout the thesis.

### 2.1 Cosmology

Cosmology today is based on observations and measurements with astronomical instruments. Due to the rapid development of technology, the knowledge of cosmology has developed significantly in recent decades. Our knowledge is therefore constantly evolving, and new observations always need to be taken into account.

Our present understanding of the Universe is based on Friedmann-Robertson-Walker (FRW) cosmology, also known as standard cosmology. This model is based on the assumption that the energy distribution of the Universe is isotropic and homogeneous, which is equivalent to considering the geometry of the Universe to be as well. This is stated by the *cosmological principle* [1]. It states that at any given instant, the Universe has the same physical properties everywhere and looks the same in all directions from every location [6, p.683]. Observations of the Universe has shown us that this assumption is valid at large scales [7]. With these assumptions, one can express the simplest metric with Cartesian coordinates to describe a system, called the FRW spacetime.

$$ds^2 = -dt^2 + a^2(t)(dx^2 + dy^2 + dz^2) \quad (1)$$

where  $a(t)$  is called the cosmic scale factor, and is a function dependent on cosmological time,  $t$ . This metric implies that all quantities are dependent on  $t$ , and not on position. Cosmological time,  $t$ , is the time considered to be starting at the Big Bang, and following the Hubble flow. Hence, cosmological time can be considered as the age of the Universe. The Hubble flow describes the movement of galaxies and astronomical objects due to the expansion of the Universe [7].

The expansion of the Universe is one of the most basic features of cosmology today. When observing the light emitted from distant galaxies, one can see that the spectra of the light from some galaxies is *redshifted* with different range. This is explained by the Doppler effect, where objects moving towards the observer emits shorter wavelengths (blueshift), and objects moving away from the observer emits longer wavelengths (redshift) [6]. These redshifts are

implying that the galaxies are moving away from the observer. Observations like these has indicated and created evidence that the Universe is expanding. The expansion was firstly discovered in the 1920s, and universality of the expansion shows us that it expands homogeneously [1] [2]. An observer, no matter where in the Universe, will always observe that all galaxies and objects are moving away from them. Redshifted galaxies and astronomical objects can be used as a probe of the Universe from early times.

The relation between redshifts measured from distant galaxies,  $z$ , and their distances from the observer,  $r$ , was recognized by the astronomer Edwin Hubble [6]. The relation is

$$z = \frac{H_0}{c} r \quad (2)$$

where  $c$  is the speed of light, and  $H_0$  is called the Hubble constant. We set today's redshift to be a zero redshift, and the redshift of the very beginning of the Universe to be an infinite redshift. The relation, (2), is called Hubble's law, and is consistent with the cosmological principle. Even though the Hubble constant is called a constant, it is actually a variable dependent on cosmological time.  $H_0$  is the value of the Hubble constant *today*, while it generally is defined as

$$H = \frac{\dot{a}(t)}{a(t)}, \quad (3)$$

where  $a$ , as mentioned previously, is the scale factor, and  $\dot{a}$  is its time derivative. The scale factor,  $a(t)$ , characterizes the Universe's expansion, and is determined by the Einstein equations.

$$\left(\frac{\dot{a}}{a}\right)^2 = \frac{1}{3M_{Pl}^2} \rho, \quad (4)$$

$$\frac{\ddot{a}}{a} = -\frac{1}{6M_{Pl}^2} (\rho + 3p), \quad (5)$$

where  $\rho$  is the energy density,  $M_{Pl}$  is the reduced Planck mass defined as  $M_{Pl} \approx 2.4 \times 10^{18}$  GeV, and  $p$  is the pressure.

The Big Bang is set to be the beginning of the Universe, at  $t = 0$ , and at this time the scale factor was zero,  $a(0) = 0$ . However, our description of the Universe is not valid until  $t_P = 5.39 \times 10^{-44}$ s, called the Planck time, and because the scale factor is negligible before this, this is considered the effective start time of the Universe [1].

There are three main types of energy in the Universe, and they have been the dominant energy form of the Universe in different eras after the Big Bang. *Radiation* was the dominant energy form from the very beginning of the Universe, and until  $z \sim 3400$ . Following this, *matter* became the dominant energy, until

$z \sim 0.3$ . From this until today,  $z \sim 0$ , the dominant energy form has been *dark energy*. Dark energy is an undefined component of negative pressure, and in the standard cosmological model it is considered to be a "cosmological constant",  $\Lambda$ . [1]

The matter density of the different eras of the Universe depends on the scale factor,  $a$ , due to the volume of the Universe expanding. It is given by the solution of the Einstein equations for the FRW metric.

$$\text{Radiation-dominated era} \Rightarrow \rho_r \propto a^{-4}$$

$$\text{Matter-dominated era} \Rightarrow \rho_m \propto a^{-3}$$

$$\Lambda\text{-dominated era} \Rightarrow \rho_\Lambda \propto \text{const.}$$

When determining  $a(t)$  in different eras from the Einstein equations, we can use the matter density. Inserting the listed values above into equation (4), we get

$$a(t) \propto t^{1/2} \text{ (radiation)} \quad (6)$$

$$a(t) \propto t^{2/3} \text{ (matter)} \quad (7)$$

$$a(t) \propto \text{const. (cosm. constant } \Lambda) \quad (8)$$

Radiation domination is the era it is believed that dark matter was produced.

We can use the matter density of different types of matter as useful cosmological parameters in the study of the Universe. A common cosmological parameter to use is  $\Omega$ . This is defined as the matter density,  $\rho$ , divided by the critical density of the Universe,  $\rho_C$ . The critical density is defined as  $\rho_C = 3H_0^2/8\pi G$  [7], and  $G$  is the gravitational constant. For instance, the cosmological parameter of the total mass in the Universe is defined as  $\Omega_0 = \frac{\rho_0}{\rho_C}$ , with  $\rho_0$  being the total mass density of the Universe today, and  $\rho_C$  is the critical density of the Universe.

In the Planck collaboration [8], they have provided values for some cosmological parameters. Listed below is the Hubble constant and the cosmological parameters of total matter, cold dark matter, baryonic matter, and the cosmological constant respectively.

$$\begin{aligned} H_0 &= 67.66 \pm 0.42 \text{ km/s/Mpc,} \\ \Omega_m &= 0.3111 \pm 0.0056, \\ \Omega_c h^2 &= 0.11933 \pm 0.00091, \\ \Omega_b h^2 &= 0.02242 \pm 0.00014, \\ \Omega_\Lambda &= 0.6889 \pm 0.0056, \end{aligned}$$

from [8], where  $h = H_0/(100 \text{ km/s/Mpc})$  is the reduced Hubble parameter [1]. For a flat Universe, not open or closed,  $\Omega_m + \Omega_\Lambda = 1$  [7]. In the case of matter contribution, the cosmological parameter,  $\Omega$ , can be referred to as the *abundance*, which is the term we will use later in this thesis in the contribution to dark matter mass.

## 2.2 Particle physics

### 2.2.1 The Standard Model

There are four fundamental forces in nature: the strong force, electromagnetic force, weak force and gravitational force. Each of these forces can be explained as interactions between elementary particles, where the interaction is caused by *field particles*. Each force has a unique field particle, also called quanta. Photons are the field particles of the electromagnetic field, gluons mediate the strong force,  $W^\pm$  and  $Z_0$  bosons are the quanta of the weak force, and the gravitational force is carried by quanta called gravitons [9, p.548]. These field particles are examples of the elementary particles with integer spin number, the bosons.

In addition to the field particles that make up the fundamental forces, there exists elementary particles that constitutes all matter. Some of these elementary particles can be affected by all four fundamental forces, while some is only affected by some of them. All the massive particles are affected by gravity, and all particles with electric charge participate in electromagnetic force [10]. Particles affected by the strong force are named hadrons, further divided into baryons and mesons. However, these particles are not considered elementary, because they are further divided into *quarks*. This includes the quarks top, bottom, up, down, charm and strange, and their antiparticles. Ordinary matter as we know it, that is visible matter, is made up of particles such as protons and neutrons. These particles go under the category of baryons, thus, we call this *baryonic matter*.

Particles affected by the weak force are named *leptons*. Leptons are considered elementary particles, and includes electrons, muons, tau particles, their corresponding neutrinos, and their antiparticles. The particles that constitutes matter, are the elementary particles that have half integer spin, hence, are the fermions.

In addition to the previously mentioned particles, there is also the anti-particles. All particles have an antiparticle, where the particle-antiparticle couple have identical mass and spin, but opposite electric charge and particle number [6]. For instance, an electron have lepton number 1, while its antiparticle, the positron,

have lepton number -1 .

Combining all these elementary particles, both the field particles and the particles that constitutes matter, we can explain the Standard Model (SM), pictured in Fig. 1. The Standard Model is a theory that combines electroweak theory, the combination of electromagnetic and weak force, and Quantum Chromodynamics (QCD). QCD is the theory of how the quarks and gluons interact by the strong force [6]. Hence, the SM includes the electromagnetic force, weak force, and strong force. The model includes all the discovered particles of matter and field particles, except the graviton, which is the quanta of the gravitational force. It also includes the Higgs boson, which is a scalar boson considered to contribute to particles having rest mass.

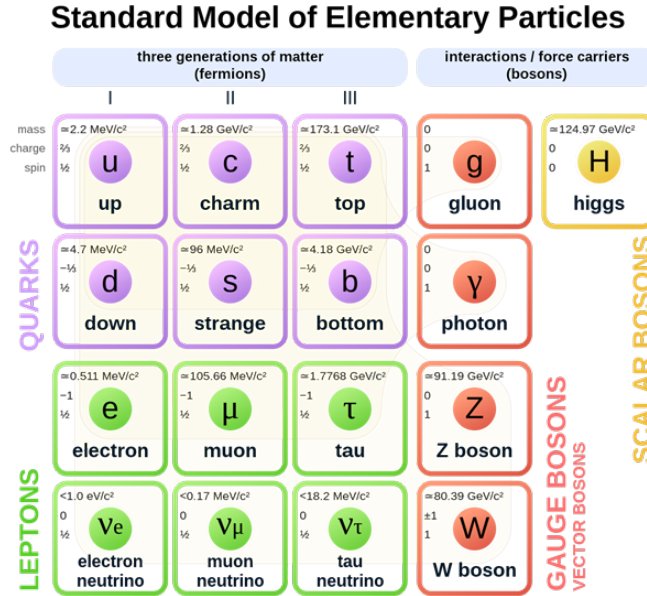


Figure 1: The Standard Model of Elementary particles. © CC BY 3.0, retrieved from [11].

### 2.2.2 Higgs mechanism

The electroweak theory proposes that the weak and electromagnetic forces have the same strength at particularly high particle energies. The two interactions are therefore looked at as the same electroweak interaction at high energies [9]. We say that at these energies the forces become symmetric, and the field particles become the same. This is the *electroweak symmetry* [9]. It states for

instance that the bosons  $W^\pm$  and  $Z^0$  are the same at high energies, but when the symmetry breaks at a certain low energy threshold, the particles gain different mass properties [9]. At normal circumstances on Earth the electroweak symmetry is broken, due to lower energy than the energy threshold.

In 1964, physicist Peter Higgs tried to explain this symmetry breaking of the electroweak theory by introducing a new field, the *Higgs field* [9]. The field particle of this field was proposed as the Higgs boson, a scalar boson. In 2012, a paper was published by CERN [12] with observations that proved the existence of the Higgs boson. The SM had included the electroweak theory, thus the discovery of the Higgs boson and the possible confirmation of Higgs mechanism, supported the SM.

The Higgs field exists in all Hilbert space, where the energy is below the symmetry breaking energy threshold. The break of the symmetry triggers the Higgs field, and particles that interact with the field, gain mass. When the particles interact with the field, one can view it as if the field causes a drag force, giving the particles their inertia [9]. Before the symmetry breaks, the weak bosons  $W^+$ ,  $W^-$  and  $Z^0$  are the same, and has no mass. When the symmetry breaks, the Higgs field contributes to give mass to the  $W^+$ ,  $W^-$  and  $Z^0$  bosons.

A simplified explanation of why this happens, is that the Higgs field in the SM, before symmetry breaking, is a special unitary doublet (SU(2)). That is, a representation of the Higgs field with two complex scalars, which corresponds to four real scalars. This is why the Higgs field has four degrees of freedom before the break of symmetry. After the symmetry breaking, three of the four degrees of freedom, or in other words, three of the four real scalars, combines with the bosons  $W^+$ ,  $W^-$  and  $Z^0$ . These scalars give the bosons their mass, leaving the field particle, the Higgs boson, with one degree of freedom, and a mass of its own at about 126 GeV [12]. This is how interactions with the Higgs field, and the Higgs boson, contributes to giving particles its rest mass.

### 2.2.3 Beyond the Standard Model

Even though the Standard Model is a good general model for many phenomena in particle physics, it does not answer all fundamental questions about particle physics [6]. The unification of the weak force and the electromagnetic force to the electroweak force, has raised the question whether one can unify the strong force and the gravitational force. Theories of unification of fundamental forces is called Grand Unification Theories (GUT). Some features of these theories are that the coupling constants of all four forces can reach a common value at some high energy [6].

The GUTs also propose a new symmetry, the *supersymmetry* (SUSY) [6]. This principle states that all the fundamental equations will be unchanged when exchanging a fermion for a boson in the equations [9]. The principle suggests that every particle has its superpartner, a *sparticle*. The sparticle of a particle is identical to the original particle in all properties, except for the difference of half a spin [6]. For instance, the superparticle of an electron, the selectron, has spin 0 although the electron has spin 1/2.

Exact supersymmetry, where the sparticle has same mass as the corresponding particle, would have already been detected if this were the case. Thus, the mass of the sparticles has to be larger, and the SUSY theory is modified so that the mass of the lightest supersymmetric particle (LSP) is of the order of the  $Z^0$  and  $W^\pm$  bosons [6].

Although no such sparticle has ever been observed, it is a theory that this symmetry is broken, hence the sparticles cannot be produced in accelerators we have access to [9]. Since the SM does not explain dark matter on its own, supersymmetry is a theory that could build onto the SM, and create a more understandable picture of the nature of dark matter. The theory of SUSY is still a thoroughly researched and tested theory, and is one of the theories they try to confirm or disprove by the use of the Large Hadron Collider (LHC) at CERN [6].

### 2.3 Statistical physics

When working in particle physics in systems where the number of particles becomes too large, to keep track on each particle, we can predict the *probable* behavior of the particles due to measurements of their macroscopic properties. When using general principles of physics on the macroscopic system, without acknowledging the motions of the individual particles, we can use *statistical* considerations to predict the probable behavior [6]. We will now look into which statistical mechanics we can use in different systems.

For a classical system where the particles are identical, but distinguishable, the distribution function of the particles is given by the Boltzmann distribution

$$f_B(E) = Ae^{-E/k_B T} \tag{9}$$

where  $E$  denotes the energy of the particle system,  $T$  the temperature, and with  $A$  as a normalization constant [6].  $k_B$  denotes the Boltzmann constant, however, we want to use natural units when calculating cosmological properties, and we have set  $k_B = 1$ . The Boltzmann distribution then reads

$$f_B(E) = Ae^{-E/T}. \tag{10}$$

In quantum mechanics, identical particles becomes indistinguishable due to the wave nature of the particles [6]. Due to this, the statistics need to be changed, and the Boltzmann distribution need to be modified. For particles with integer spin, bosons, we use the Bose-Einstein distribution

$$f_{BE}(E) = \frac{1}{e^\alpha e^{E/T} - 1} \quad (11)$$

where  $e^\alpha$  replaces the normalization constant  $A$ , and  $\alpha = -\frac{\mu}{T}$  [6].  $\mu$  is the chemical potential of the particle system. For particles with half-integer spin, fermions [6], we use the Fermi-Dirac distribution

$$f_{FD}(E) = \frac{1}{e^\alpha e^{E/T} + 1}. \quad (12)$$

Combining the two different distributions into a general one, and simplifying the term, we can express the distribution we are going to use in the calculations of DM particles as

$$f_i(E) = \left[ e^{(E-\mu_i)/T_i} \mp 1 \right]^{-1}, \quad (13)$$

where  $i$  denotes the particle species, and the minus and plus sign are for whether the particle species are bosons or fermions, respectively.

Equation (13) is also known as the corresponding distribution function of the Grand Canonical Ensemble (GCE). This function describes a system in thermal equilibrium where the particles in the system is interacting weakly with a large reservoir, and where the particle number and total energy is constant [7].

The relation between the distribution of a particle species  $i$  in a system,  $f$ , and the particle density number,  $n_i$ , can be expressed as

$$n_i(t) = \frac{g}{(2\pi)^3} \int d^3p f_i(E, t), \quad (14)$$

where  $p$  is the momentum of the particles, and  $g$  is the degrees of freedom [7].

Total radiation density for the radiation dominated era are given by

$$\rho_r = \frac{\pi^2}{30} g_* T^4. \quad (15)$$



## 2.4 DarkSUSY

DarkSUSY is an advanced tool to calculate dark matter properties numerically [5]. This program uses Fortran code to calculate wanted properties for several DM particle candidates, and different DM production mechanisms. The program can for instance, from the choice of some properties, calculate the relic abundance of DM, and much else.

In this thesis we use DarkSUSY 6, which was released in 2018 [5]. Even though the SUSY in DarkSUSY is short for supersymmetry, the program includes computations for non-supersymmetric DM particle models too. The program has modules for different DM particle models, and example programs for specific calculations we can use with them. In this thesis we will mainly use the `generic_wimp` module, and `silveira_zee` module. We will describe these modules in more details when using them later. We will use example programs for both the freeze out and freeze in production mechanisms.

When modifying example programs, we will add some details of the modification in the Appendix.

## 3 Evidence for dark matter

In this section, we will review some details of how physicists came to think that the Universe largely consisted of some invisible form of matter, and how they eventually found evidence of this. We will look at the two main observations of galaxies and galaxy clusters that indicates the existence of dark matter, in addition to the cosmic microwave background radiation. Further, we will review what we know of the nature of dark matter.

### 3.1 Early history

In 1687, Isaac Newton published his explanation of the gravitational motion of astronomical objects. This was a theory proposed on the basis of astronomical observations, and intuitive logic. This theory allowed physicists to predict the motion of astronomical objects. However, in some cases, the astronomical objects did not follow the path the physicists had predicted. Because the Newtonian gravitation law successfully explained other phenomena in the Universe, the physicists began to wonder why it failed to predict the motion of certain astronomical objects. The deviations from the expected gravitational motion of astronomical objects, led to the suspicion that there could be objects in the Universe one could not see. [13]

This suspicion grew stronger when the explanation that there were “dark” objects in the Universe, could be used to predict the existence of unseen astronomical objects, such as planets. The astronomers U. Le Verrier and John C. Adams could use this theory to predict the existence of the planet Neptune, which was eventually discovered in 1846 [2]. This discovery was also an important confirmation of the accuracy of the Newtonian gravity. When physicist learned that there could be objects or matter in the Universe one could not see, it opened their eyes to a new view of the Universe. The deviations of the gravitational motion of objects in the Universe, led to theories that there could exist some type of dark matter out there. However, some physicist believed that the reason for the deviations of gravitational motion, was because the gravitational laws as they knew them, did not apply for such large scales [13]. To be able to validate the different theories, more refined laws of gravitational motion were necessary. This would have to wait until Einstein’s theory of general relativity was proposed in 1916. [13]

The astronomer Fritz Zwicky developed the theory of dark matter further, by proposing that this undiscovered matter was a pervasive fluid-like matter that would compile to, and make up the most of, astronomical systems like galaxies and galaxy clusters [2]. This proposal was not well received at first, and it took

about 40 years for this theory to be accepted [2].

Zwicky was a physicist ahead of his time, and made important observations and theories of the evolution of stars, and contributions to classifications of galaxies and clusters of galaxies [2]. He was the one who discovered that the galaxies in the Coma cluster, a large galaxy cluster discovered in 1656, was moving too fast due to their visible mass [14]. Observations had shown that the galaxies in the cluster had a Doppler effect of 1000 km/s or more [15], which did not correspond to the density of the visible mass of the galaxies. For this redshift to be correct, the average density of the Coma cluster would have to be at least 400 times larger than what the visible matter contributed to. This indicated that the cluster consisted of much more matter than what the astronomers first had thought, and that most of the matter would not be visible. This is considered the first breakthrough in the history of dark matter, and in the following years several other observations could also be explained by the theory of dark matter. [2] [13] [14] [15]

### 3.2 Observational evidence

Even though dark matter cannot be observed by the naked eye, there have been measurements that have detected dark matter in the Universe. With Zwicky's discovery of the galaxy movement in the Coma cluster being the first breakthrough of the knowledge of dark matter, the theory started to be more and more experimented and tested.

The evidence of the existence of dark matter relies on observations of gravitational effects. The most unexpected gravitational effects can be measured from galaxies, and particularly spiral galaxies. A spiral galaxy is typically shaped as a disc, with a bulge in the center. The visible mass of this galaxy is gathered in the bulge and the disc, and the disc fades away far from the center. [1]

Using Newtonian gravitational theory, and assuming that the Newtonian gravitational force,  $g_n$ , provides the centripetal acceleration of the spiral galaxy, we have

$$g_n = \frac{v^2}{r} \quad (16)$$

where  $g_n$  is defined as

$$g_n = \frac{G M}{r^2}. \quad (17)$$

When combining these equations, we can see that the rotation velocity at distance  $r$  from the center of the galaxy is

$$v(r) = \sqrt{\frac{GM}{r}} \quad (18)$$

where  $M$  is the mass in a sphere with corresponding radius  $r$ . As the distance  $r$  increases, the rotational velocity decreases. From this formula one would expect the rotational velocity to decrease the farther out we would go, until the velocity got to zero. However, observations show us that this is not the case. [1]

Observations of rotational velocity of the galaxy M31, also known as the Andromeda galaxy, showed that the rotational velocity of the galaxy remained equal at inner regions of the galaxy, as the outer regions [16] [17]. This was the case for distances of almost twice the length of where starlight could be detected. This tells us that the rotational velocity of a spiral galaxy increases until a certain point far from the center, where the velocity approximately becomes constant. When considering the constant rotational velocity within radius  $r$ , the mass  $M$  inside this radius is not set to be constant, but a function of the distance from the galaxy center. It is set to be

$$M(r) = \frac{rv_c^2}{G}. \quad (19)$$

When  $r$  increases, we see that  $M$  increases too. This indicates that the mass increases beyond the visible disc, which means that there is invisible mass beyond the visible mass. This invisible mass is considered to mainly come from dark matter. For the study of elliptic galaxies this is also the case, and when studied globally, dark matter represents approximately 80-90% of all galaxies. [1]

Another measurement that can be seen as evidence of the existence of dark matter is the weight of galaxy clusters. A galaxy cluster is a cluster of galaxies bound together by gravity. This massive object contains large amounts of gas. To determine the mass of galaxy clusters, as well as objects in the Universe in general, we can use *gravitational lensing* methods. This is a phenomenon where a galaxy far away emits light, and there is a massive object between the galaxy and the observer. In this case the massive object between them, is a massive galaxy cluster. The gravitational pull of the galaxy cluster pulls the light emitted from the galaxy, causing the light to bend its trajectory. By looking at how the light is bent on its way to the observer, we can estimate the mass of the galaxy cluster. [1]

A gravitational lens has no focal point, but rather a focal line we refer to as the Einstein circle. This is because the light will be shaped as a ring around the massive object, if the galaxy emitting the light is located directly behind it. If not, the observer will see an uncomplete circle, and many distorted images of the galaxy. [1]

Distant galaxies behind a galaxy cluster create strong gravitational lensing. This causes many distorted images to appear spread on the Einstein circle. The radius of this Einstein circle is related to the mass of the galaxy cluster, so we can determine the mass of the cluster by looking at its gravitational lensing. The angular radius of the Einstein circle,  $\theta_E$ , is expressed by

$$\theta_E = \sqrt{\frac{4GM}{c^2} \frac{(D_S - D_L)}{D_S D_L}}. \quad (20)$$

$M$  is the galaxy clusters mass,  $D_L$  is the distance from the observer to the gravitational lens, and  $D_S$  is the distance from the observer to the light source. From this relation we can determine the mass of the galaxy cluster by the use of the gravitational constant  $G$ , and the distances to the lens and source. [1] When calculating this, physicists noticed that the visible mass only contributes to about 10-20% of the calculated mass. Doing several observations and calculations of this, it confirmed that approximately 80-90% of the mass of galaxy clusters are invisible and correspond to dark matter, the same results as for galaxies. [1]

Cosmic microwave background (CMB) radiation is an important source of data from which we can study the early Universe, and most of the information we know about DM, among it the relic abundance, actually come from the study of CMB.

After the Big Bang, the Universe was made up of significantly many charged particles, creating an ionized gas known as *plasma*. The plasma was so hot and dense that all the particles collided with each other at such high rates that no neutral atoms were able to be made, and no particles could escape the plasma. As the Universe expanded, and thus cooled, the plasma eventually managed to get low enough energy to let charged particles create neutral atoms. This was about 370 000 years after the Big Bang, and this is known as the *recombination epoch* [1]. This eventually allowed photons to travel through the Universe, leading to the electromagnetic radiation known today as CMB. [1]

Since CMB originated from the early Universe, this can give us a lot of information about structures and densities throughout the Universe. This is done by measurements of the radiation, and that is where the properties known from the Planck collaboration was discovered [8]. Hence, it is from CMB we get the cosmological parameters listed in section 2.1.

### 3.3 Nature of dark matter

Ever since evidence of dark matter was discovered, the identity of what particle or particles it is composed of has been a mystery. However, due to observations, indications have grown that our Standard Model does not include any type of particle that can have the characteristics of a dark matter particle. Thus, we think that dark matter is composed of an unknown type of matter. In this section, we will look into the nature of dark matter, and which characteristics the DM particles need.

One of the most groundbreaking observations revealing the nature of dark matter, was the observation of a bullet cluster in 2006. A bullet cluster is two galaxy clusters colliding with each other. The gravitational lensing of the cluster showed that the gravitational potential of the two clusters did not trace the plasma, as expected if all the matter was composed of continuously the same baryonic particles. Due to the plasma being the dominant substance of baryonic matter in the Universe, and the disorientation of the gravitational potential being too large, this implied that the majority of matter in the bullet cluster were not baryonic. The groundbreaking discovery was that the majority of matter, the dark matter, was spread away from the plasma, which proved that dark matter and baryonic matter consists of different entities with different properties. This discovery also disproved that the reason for the deviations of gravitational motion was due to modified gravitational laws for larger scales, as some physicists still wondered could be the case. [1] [3]



Figure 2: The bullet cluster. The red-coloured mass is the visible mass composed of hot gas. The blue-coloured mass is the invisible mass, that has been deduced from gravitational lensing. © 2021 Elsevier B.V. All rights reserved. Retrieved from [1], with permission.

Fig. 2 shows us that the visible mass (red) and the invisible mass (blue) has not interacted. The visible mass, corresponding to the hot gas, has experienced a drag force due to interactions in the collision. This is what creates its bullet shape. However, the invisible mass has not experienced this, thus has been separated from the hot gas. This shows us, as mentioned earlier, that the dark matter does not interact with baryonic matter. Due to baryons interacting with each other, this indicates that DM is a *non-baryonic* matter, and most likely are weakly self-interacting as well. This also indicate that the particles do not have any electrical charge. [1]

If indeed dark matter consists of new particles, we want to know whether the particles have relativistic or non-relativistic velocities. It is common to denote dark matter with relativistic and non-relativistic velocities, "hot" and "cold" respectively. As the dark matter particles do not interact with baryons and have no electric charge, there is only the neutrino in the SM that can have the characteristics of a dark matter particle. However, since the neutrino is a quite light particle, it will travel with relativistic velocity. Thus, the neutrino can act as a good candidate for hot dark matter, but not for cold.

Hot dark matter, due to the high velocity of the particles, will spread structures in a different way than what we observe. Also, the CMB would have different properties if hot dark matter would have interfered. This indicates that hot dark matter can only make up a fraction of the total dark matter, and most of the DM therefore consists of cold DM. In this thesis we will assume that all

dark matter is cold. [1]

For the particles to have non-relativistic velocities, they have to have a large mass. A massive particle is the best particle candidate to fit the characteristics of the cold dark matter particle. [5]



## 4 Thermal freeze out of dark matter

There are several theories of where DM comes from, or how it is produced. In this section, we will look into one of the most studied models of DM production, the thermal freeze out of DM. We will firstly explain what the phenomenon is, and then look into the thermodynamic properties of the particles when this occurs. All the derivations we do in this section are based on derivations from Kolb and Turners book *Early Universe*, reference [7].

In the early Universe, it is assumed that most elements of the Universe were in a thermal equilibrium. Even though this is strictly not possible, due to, among other things, the expansion of the Universe, the Universe has throughout its history been nearly in thermal equilibrium. Thus, describing the Universe this way is a quite good approximation. In the equilibrium, the particles interact without transferring any net energy between them. As the Universe expands, particles can deviate or decouple from the thermal equilibrium. When a particle species decouples from the equilibrium, relics are made, which can be thoroughly studied. The properties of these relics can give a lot of information about the particle species it consists of, and this is used especially with the study of dark matter. When a particle species decouples from the thermal equilibrium, we say that they *freeze out*. It is assumed that the freeze out of DM happened in the radiation-dominated era.

In order to decouple from the thermal equilibrium, the particles need to have an interaction rate lower than the expansion of the Universe. That is, the expansion rate,  $H$ , has to exceed the interaction rate,  $\Gamma$ .

$$\Gamma \gtrsim H \tag{21}$$

$$\Gamma \lesssim H \tag{22}$$

In (21), the particles with interaction rate  $\Gamma$ , will still be coupled to the thermal equilibrium, while in (22) the particles may have decoupled. We will see later that this holds.

### 4.1 Boltzmann equation

As mentioned in section 2.3, the distribution function of a particle species in *thermal equilibrium* can be expressed by the distribution function corresponding to the GCE, equation (13). We can use this distribution for the particles in the thermal equilibrium of the early Universe, because we make the approximation

that the Universe is the large reservoir the particles interact with. Even if the Universe is expanding, this is a valid approximation. For the thermal equilibrium of the early Universe,  $T_i$  in equation (13) is just set to be the temperature of the equilibrium,  $T$ , and  $\mu_i$  is some chemical potential. [7]

When wanting to express the *decoupling* from the thermal equilibrium, one has to take into account deviations in the GCE distribution. It is described by the Boltzmann equation of the form

$$L[f_i] = C[f_i, \{f_i\}] \quad (23)$$

where  $f_i = \xi(t)f_{ieq}$ , and  $\xi(t)$  is a function depending on cosmological time,  $t$ . The left-hand side of equation (23) contains the Liouville term, while the right-hand side has the collision terms of the interacting particles [7]. The Liouville term for a FRW metric is

$$L[f_i(t, E)] = E \frac{\partial f_i}{\partial t} - \frac{\dot{a}}{a} |\vec{p}|^2 \frac{\partial f_i}{\partial E} \quad (24)$$

Considering this equation, and the number density of the decoupling particle species  $i$ , from equation (14) in section 2.3, we can integrate by parts and get the result for the Boltzmann equation

$$\frac{dn_i}{dt} + 3Hn_i = \tilde{C}[f_i] \quad (25)$$

where  $\tilde{C}$  is the new collision term. When evaluating the collision term, we need to consider all the particle interactions in the equilibrium that contribute to change in the dark matter particle number. For the process of  $\chi + a + b \dots \leftrightarrow i + j \dots$ , the contributions to the collision term are

$$\begin{aligned} \Delta \tilde{C} = & - \int (d\Pi_\chi d\Pi_a d\Pi_b \dots) (d\Pi_i d\Pi_j \dots) (2\pi)^4 \\ & \delta^{(4)}((p_\chi + p_a + p_b + \dots) - (p_i + p_j \dots)) \\ & \times \frac{1}{S} \left[ |\tilde{M}_{\chi+a+b \dots \rightarrow i+j \dots}|^2 f_\chi f_a f_b \dots (1 \pm f_i)(1 \pm f_j \dots) \right. \\ & \left. - |\tilde{M}_{i+j \dots \rightarrow \chi+a+b \dots}|^2 f_i f_j \dots (1 \pm f_\chi)(1 \pm f_a)(1 \pm f_b) \dots \right], \quad (26) \end{aligned}$$

where  $S$  is a symmetry factor, taking into account that there can be multiple particles of the same species in the final state.  $\delta$  corresponds to the delta function, and  $|\tilde{M}_{i \dots \rightarrow a \dots}|$  is the matrix for the specific process. The plus and minus sign corresponds to the particle species being bosons and fermions respectively,

and  $d\Pi_i$  is expressed as

$$d\Pi_i = \frac{g_i}{(2\pi)^3} \frac{d^3 p_i}{2E_i}. \quad (27)$$

To simplify this complicated collision term, we can make some approximations. Assuming there is no Fermi degeneracy or Bose-Einstein condensate, which is a valid assumption for the cases we are most interested in, we use the Maxwell-Boltzmann statistics for all species in the equilibrium. Thus, we use the same distribution function for the bosons and fermions. By taking  $f_i \ll 1$ , we get  $(1 \pm f_i) \simeq 1$ . We can also assume that violations of the charge and parity symmetry (CP) are small, which means that the process and back-process are approximately equal,  $|\tilde{M}_{\chi+a+b.. \rightarrow i+j..}|^2 \simeq |\tilde{M}_{i+j.. \rightarrow \chi+a+b..}|^2 = |\tilde{M}|^2$ . These approximations simplify equation (26), so that we can write the Boltzmann equation as

$$\begin{aligned} \frac{dn_i}{dt} + 3Hn_i = & - \int (d\Pi_\chi d\Pi_a d\Pi_{b..}) (d\Pi_i d\Pi_{j..}) (2\pi)^4 |\tilde{M}|^2 \\ & \delta^{(4)}((p_\chi + p_a + p_b + ..) - (p_i + p_{j..})) [f_\chi f_a f_{b..} - f_i f_{j..}]. \end{aligned} \quad (28)$$

This is the Boltzmann equation describing the particle decoupling from the thermal equilibrium.

## 4.2 Applications of the Boltzmann equation

By looking at specific applications of the Boltzmann equation, we can treat thermodynamics of the thermal freeze out of dark matter. To do this, we need to make some assumptions. We assume that dark matter is made of one single species of particles, and that these particles are protected by a new symmetry such that new particles are always produced in pairs [1]. We set the reaction that changes the number of dark matter particles before the freeze out, to be of the form  $\chi\bar{\chi} \leftrightarrow f\bar{f}$ , where we denote the DM particles with  $\chi$ , and  $f$  is a fermion included in the Standard Model. This will be the case if  $\chi$  is a stable particle species. We also assume that the dark matter particle is its own antiparticle,  $\bar{\chi} = \chi$ , then their chemical potential will be zero,  $\mu = 0$ . For this process, the collision term in the Boltzmann equation will be

$$\Delta\tilde{C} = - \int (d\Pi_{\chi_1} d\Pi_{\chi_2}) (d\Pi_f d\Pi_{\bar{f}}) (2\pi)^4 \delta^{(4)}(\dots) |\tilde{M}|^2 \left(\frac{1}{2} \times 2\right) (f_{\chi_1} f_{\chi_2} - f_f f_{\bar{f}}) \quad (29)$$

The factor 2 explains that the number of dark matter particles changes by two units in this specific reaction, but it is cancelled by the fact that the dark matter particles are identical, ( $\bar{\chi} = \chi$ ), and the symmetry factor is  $\frac{1}{2}$  [7]. If we consider the last part in the collision term, ( $f_{\chi_1} f_{\chi_2} - f_f f_{\bar{f}}$ ), we can simplify this by consider that both  $\chi$  and  $f$  has zero chemical potential,  $\mu_i = 0$ . If we also assume that  $f$  and  $\bar{f}$  are in the thermodynamic equilibrium, we can use the approximation ( $1/(e^{E/T} \mp 1) \simeq e^{-E/T}$ ) for the distribution functions. This simplifies the expressions

$$\begin{aligned} f_f &= e^{-E_f/T} \\ f_{\bar{f}} &= e^{-E_{\bar{f}}/T} \end{aligned} \quad (30)$$

The energy part of the  $\delta$ -function in the collision term (29), gives that  $E_\chi + E_\chi = E_f + E_{\bar{f}}$  [7]. Considering this, and the two equations (30), we see that

$$f_f f_{\bar{f}} = e^{-(E_f + E_{\bar{f}})/T} = e^{-(E_\chi + E_\chi)/T} = f_{\chi_{eq}} f_{\chi_{eq}} \quad (31)$$

From this, it follows that

$$f_\chi f_\chi - f_f f_{\bar{f}} = f_\chi f_\chi - f_{\chi_{eq}} f_{\chi_{eq}} \quad (32)$$

Now we can write the collision term in terms of  $n_\chi$ , the actual number density of the dark matter particles, and  $n_{\chi_{eq}}$ , the number density of dark matter particles in thermal equilibrium [7]. We use the definition of the number density defined in section 2.3, equation (14). We get

$$\Delta \tilde{C} = -\langle \sigma v \rangle (n_\chi^2 - n_{\chi_{eq}}^2), \quad (33)$$

where  $\langle \sigma v \rangle$  is the thermal average of the annihilation cross section multiplied with the relative velocity of incoming particles, calculated from  $|\tilde{M}|^2$ . For simplicity,  $\langle \sigma v \rangle$  will be referred to as *average* (annihilation) cross section in this thesis, while  $\sigma$  is the cross section. The Boltzmann equation then reads

$$\frac{dn_\chi}{dt} + 3Hn_\chi = -\langle \sigma v \rangle (n_\chi^2 - n_{\chi_{eq}}^2). \quad (34)$$

This is the Boltzmann equation we want to work with. However, to make calculations easier, and to simpler study the thermodynamics of the dark matter freeze out, we define some useful variables. We define the yield variable to be

$$Y_\chi = \frac{n_\chi}{s}, \quad (35)$$

where  $n_\chi$  is the number density of the dark matter particles, and  $s$  is the entropy

density of the thermal plasma. Due to the conservation of entropy per comoving volume,  $sa^3 = \text{const.}$ , and the fact that  $n_\chi$  scales with  $a$  in the same way as the entropy density, the yield variable will remain approximately constant after the freeze out [7]. Then it also follows that

$$\frac{dn_\chi}{dt} + 3n_\chi H = s \frac{dY_\chi}{dt}. \quad (36)$$

By inserting (35) for  $n_\chi$  in equation (34), we get

$$\frac{d(Y_\chi s)}{dt} + 3HY_\chi s = -\langle\sigma v\rangle s^2 (Y_\chi^2 - Y_{\chi eq}^2). \quad (37)$$

which we can rewrite, due to relation (36), to be

$$\frac{dY_\chi}{dt} = -\langle\sigma v\rangle (Y_\chi^2 - Y_{\chi eq}^2). \quad (38)$$

Further we define a new convenient variable,

$$x = \frac{m_\chi}{T}. \quad (39)$$

We want to exchange the time dependence in equation (38) with dependence on  $x$ , such that we get the temperature dependence through this factor. This is convenient because  $x$  is a dimensionless variable. To exchange the dependence from  $t$  to  $x$ , we use a Hubble relation for the radiation dominated era. This is obtained when combining (4), (6) and (15).

$$H^2(t) = \left(\frac{1}{2t}\right)^2 = g_* \frac{\pi^2}{90} \frac{1}{M_{Pl}^2} T^4 = H^2(T) \quad (40)$$

From this we get the expression for  $t(x)$ . By the use of (39), (40), and the fact that  $\frac{dY_\chi}{dt} = \frac{dY_\chi}{dx} \frac{dx}{dt}$ , we can express the Boltzmann equation (38) as

$$\frac{dY_\chi}{dx} = -\frac{s\langle\sigma v\rangle}{H(T)} \frac{1}{x} (Y_\chi^2 - Y_{\chi eq}^2) \quad (41)$$

The Hubble constant when we assume that  $T = m_\chi$ ,  $H(m_\chi)$ , is related to the  $H(T)$  by  $H(T) = H(m_\chi)x^{-2}$ . When using this relation, we get the final expression for the Boltzmann equation for the cosmological evolution

$$\frac{dY_\chi}{dx} = -\frac{xs\langle\sigma v\rangle}{H(m_\chi)} (Y_\chi^2 - Y_{\chi eq}^2) \quad (42)$$

From the very convenient form of the Boltzmann equation we now have derived, we can study more in detail when a freeze out occurs [7]. We can express equation (42) in a suggestive way,

$$\frac{x}{Y_{\chi_{eq}}} \frac{dY}{dx} = -\frac{\Gamma}{H} \left[ \left( \frac{Y_{\chi}}{Y_{\chi_{eq}}} \right)^2 - 1 \right]. \quad (43)$$

Where  $\Gamma$  is the interaction rate of all annihilation channels before the freeze out, and is given by

$$\Gamma = n_{eq} \langle \sigma v \rangle, \quad (44)$$

From (43) we can see that the freeze out will occur approximately when  $\Gamma \simeq H \simeq n_{eq} \langle \sigma v \rangle$ . This supports the statement earlier from equation (21) and (22), that when  $\Gamma \geq H$  the particles are still coupled to the equilibrium, but for  $\Gamma \leq H$  the particles will in theory have decoupled.

When we know that freeze out of interactions happens at approximately  $\Gamma \simeq H$ , we can estimate a value for  $x$  when the freeze out happens, if we assume that the particles are non-relativistic during the freeze out. This will also estimate the temperature of when the freeze out will occur,  $x_{fo} = \frac{m_{\chi}}{T_{fo}}$ . The estimated value for  $x_{fo}$  when  $H \simeq \kappa n_{eq} \langle \sigma v \rangle$  is

$$x_{fo} = \ln \left[ \kappa \sqrt{\frac{90}{8\pi^3}} \left( \frac{g_{\chi}}{\sqrt{g_*}} \right) m_{\chi} M_{Pl} \sigma_n \right] - (n+1) \ln \left( \ln \left[ \kappa \sqrt{\frac{90}{8\pi^3}} \left( \frac{g_{\chi}}{\sqrt{g_*}} \right) m_{\chi} M_{Pl} \sigma_n \right] \right) \quad (45)$$

This is a modified version of an equation retrieved from [7].  $\kappa$  is a constant of unity, and a good approximation is  $\kappa = (n + 1)$ . We also use the assumption that  $\langle \sigma v \rangle \simeq \sigma_n x^{-n}$ . Equation (45) shows us that the freeze out  $x$  only depend logarithmically on the dark matter mass,  $m_{\chi}$ .

### 4.3 Relic abundance in case of thermal freeze out

When particle interactions freeze out of the thermal equilibrium, the particle relics create an abundance of the particle species, the *relic abundance*. The relic abundance is an important observable used to determine characteristics of dark matter [1]. If the dark matter particles had been in equilibrium from the early Universe until today, we could neglect its relic abundance. However, if the particle interactions freeze out when the temperature is such that  $x_{fo} = m_{\chi}/T_{fo}$  is barely larger than 1, the species will have a significant relic abundance [7].

From the Boltzmann equation (42) we derived in section 4.2, we can further

derive an expression for the relic abundance of dark matter,  $\Omega_\chi$ . We want to find an approximation for the region  $x \gg x_{fo}$ , where it follows that  $Y_\chi \gg Y_{\chi_{eq}}$ , since this will occur *after* the freeze out [7]. Then we can neglect the  $Y_{\chi_{eq}}$  term in equation (42), and we get

$$\frac{dY_\chi}{dx} = -\frac{xs\langle\sigma v\rangle}{H(m_\chi)} Y_\chi^2 \quad (46)$$

By using the definition of the entropy,

$$s(x) = g_{*s} \frac{2\pi^2 m_\chi^3}{45x^3}, \quad (47)$$

and assuming  $\langle\sigma v\rangle \simeq \sigma_n x^{-n}$ , we get

$$\frac{dY_\chi}{dx} = -\lambda \sigma_n x^{-(n-2)} Y_\chi^2 \quad (48)$$

where  $\lambda = \frac{2g_{*s}\pi^2 m_\chi^3}{45H(m_\chi)}$ . The relation  $\langle\sigma v\rangle \simeq \sigma_n x^{-n}$  shows us that when  $n = 0$ ,  $\langle\sigma v\rangle$  is constant, which we will use later in the case of a generic WIMP model. When solving (48) analytically, by integrating  $x$  from  $x_{fo}$  to  $x_0 \approx \infty$ , we find that

$$Y_\chi = \frac{(n+1)x_{fo}^{(n+1)}}{\lambda\sigma_n} \quad (49)$$

To get from the yield function to the relic abundance we need to multiply by  $\frac{m_\chi s_0}{\rho_c}$ , due to the definition of abundance in section 2.1, where  $s_0$  is the entropy density of today.

$$\Omega_\chi = \frac{(n+1)x_{fo}^{(n+1)} m_\chi s_0}{\lambda\rho_c\sigma_n} \quad (50)$$

When converting back from  $\langle\sigma v\rangle \simeq \sigma_n x^{-n}$ ,  $\lambda = \frac{2g_{*s}\pi^2 m_\chi^3}{45H(m_\chi)}$  and  $H(T) = H(m_\chi)x^{-2}$ , we end up with the result

$$\Omega_\chi \simeq \left( \frac{45s_0}{2\sqrt{90}\pi\rho_c} \right) \frac{(n+1)x_{fo}}{\langle\sigma v\rangle M_{Pl} \frac{g_{*s}}{\sqrt{g_*}}} \quad (51)$$

where  $s_0$  and  $\rho_c$  are constants defined as  $s_0 \simeq 3000 \text{ cm}^{-3}$  and  $\rho_c \simeq (1.05h^2) \times 10^4 \text{ eVcm}^{-3}$ , where  $h$  is the reduced Hubble parameter defined in section 2.1. We can express this in a more convenient way,

$$\Omega_\chi h^2 \simeq \left( \frac{45s_0}{2\sqrt{90}\pi \frac{\rho_c}{h^2}} \right) \frac{(n+1)x_{fo}}{\langle\sigma v\rangle M_{Pl} \frac{g_{*s}}{\sqrt{g_*}}}, \quad (52)$$

where the first term in the parenthesis is all constants. From this result we see

that the relic abundance is not dependent on any of the properties of the SM particle the dark matter particle annihilates into. Also, it is only dependent logarithmically on the dark matter particle mass, due to the approximation of  $x_{fo}$  in equation (45).

## 4.4 DarkSUSY results

In this section, we will use DarkSUSY to do calculations of dark matter properties, and compare them with the approximate formulas we have derived and with the observed values from the Planck collaboration [8]. We will do this mainly by the use of the `generic_wimp` module in the program. We will still assume that the annihilation process is of the form  $\chi\chi \leftrightarrow f\bar{f}$ .

### 4.4.1 The generic WIMP module

For cold dark matter, the appropriate DM particle candidate need to *massive*, as mentioned in section 3.3. Equation (52) show us that the average annihilation cross section of DM,  $\langle\sigma v\rangle$ , need to be very small, hence the particles are interacting *weakly*. This can be shown in (52) by inserting  $\Omega_\chi h^2 \approx 11933$  from [8],  $g^*$  and  $g_{*s}$  from [18], and the Planck mass  $M_{Pl} \approx 2.4 \times 10^{18}$  GeV. Assuming  $n = 0$ ,  $x_{fo}$  is the only missing property, which we can get from (45). We will do calculations with this formula and properties later, with the help of DarkSUSY.

Such a weakly interacting massive particle (WIMP), is a good particle model for DM particles from the freeze out production mechanism. This will be the particle model we use when doing calculations of DM properties in DarkSUSY.

The `generic_wimp` module in DarkSUSY is made to demonstrate how DarkSUSY can be used to calculate simple WIMP dark matter. By only inserting a minimum of parameters in the program, one can get results and properties of a WIMP dark matter. The parameters we need to input are the wanted dark matter mass,  $m_\chi$ , a constant  $\langle\sigma v\rangle$ , the spin-independent scattering cross-section of dark matter with nucleons,  $\sigma_{SI}$ , and whether the dark matter particle is its own anti-particle or not [5]. We also need to specify the dominant annihilation channel.

To do further calculations, the `generic_wimp` module is quite straightforward to modify to get the wanted properties. We will mainly use the `generic_wimp` module to get our wanted properties, and also modify some of the example programs in DarkSUSY. The modifications we do, will be described in Appendix B.



#### 4.4.2 Calculations of relic abundance

From the observational results from the Planck collaboration, we know that the relic abundance of cold dark matter is  $0.11933 \pm 0.00091$  [8]. By the use of DarkSUSYs generic\_wimp module, we can calculate what order of average cross section,  $\langle\sigma v\rangle$ , the particle interactions should have, that corresponds to this observed quantity. By modifying the dsmain\_wimp example program in the generic\_wimp module, we get corresponding values for the relic abundance considering the dark matter particles mass, if we set the average cross section to be constant. We try for the neutrino as annihilation channel, and set the average cross section to be  $1 \times 10^{-25} \text{ cm}^3\text{s}^{-1}$ ,  $1 \times 10^{-26} \text{ cm}^3\text{s}^{-1}$  and  $1 \times 10^{-27} \text{ cm}^3\text{s}^{-1}$ . For more detailed explanation of the modifying of programs see Appendix B.

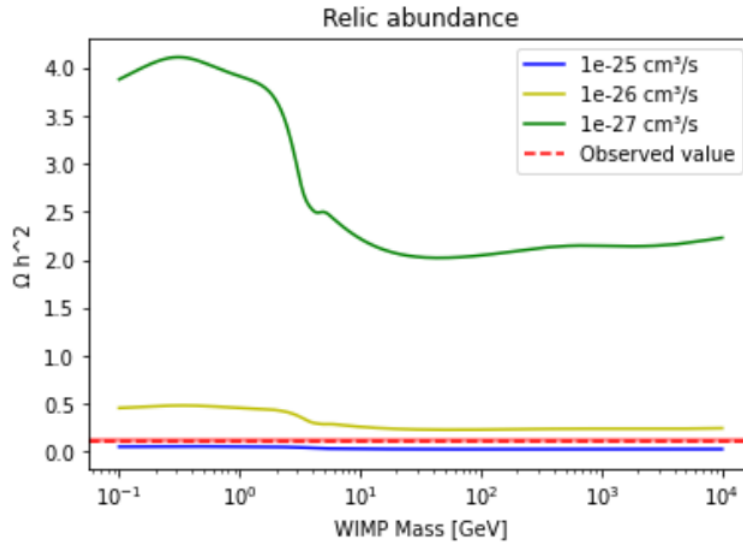


Figure 3: The relic abundance of neutrinos with average cross section  $1 \times 10^{-25} \text{ cm}^3\text{s}^{-1}$ ,  $1 \times 10^{-26} \text{ cm}^3\text{s}^{-1}$  and  $1 \times 10^{-27} \text{ cm}^3\text{s}^{-1}$ . The red line represents the observed relic abundance from the Planck collaboration, with  $3\sigma$  error.

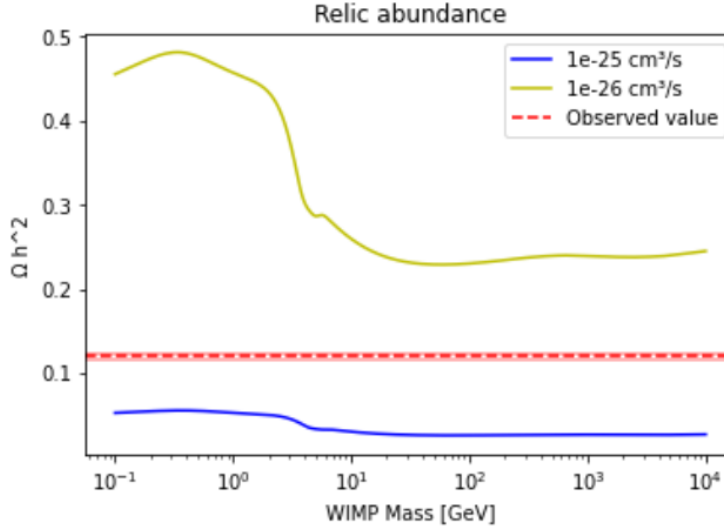


Figure 4: The relic abundance of neutrinos with average cross section  $1 \times 10^{-25} \text{ cm}^3\text{s}^{-1}$  and  $1 \times 10^{-26} \text{ cm}^3\text{s}^{-1}$ . The red line represents the observed relic abundance from the Planck collaboration, with  $3\sigma$  error.

From Fig. 3, we see that average cross sections  $1 \times 10^{-25} \text{ cm}^3\text{s}^{-1}$  and  $1 \times 10^{-26} \text{ cm}^3\text{s}^{-1}$ , are the values that creates a relic abundance closest to the observed value. However, if we zoom the plot, Fig. 4, we can see that none of the chosen average cross sections actually creates a relic abundance that intersects the observed relic abundance. This means that none of these values for the average cross section can be correct for the observed value. We also tried the same average cross sections for the muon, but this gave the same results, as previously expected from equation (52) in section 4.3, and thus created the same plot.

To try to get the correct average cross section, such that it creates a relic abundance similar to the observed value, we can try with other values for the average annihilation cross section.

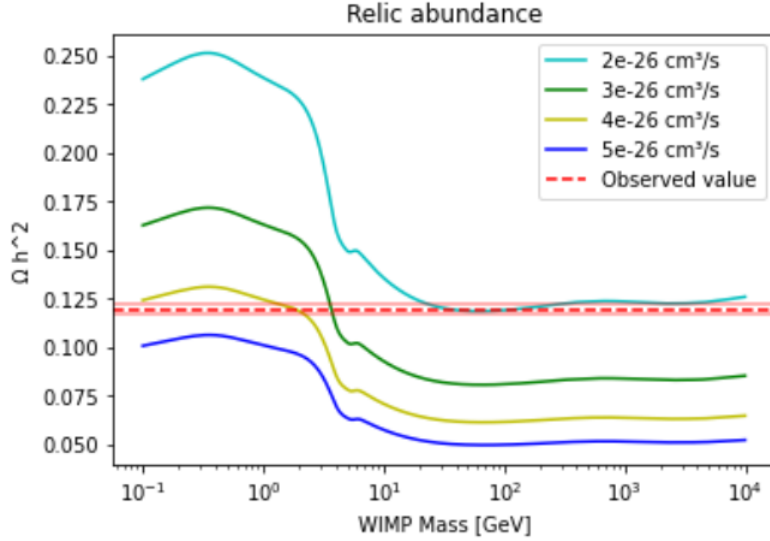


Figure 5: The relic abundance with neutrino as annihilation channel and average cross section set to be  $2 \times 10^{-26} \text{ cm}^3\text{s}^{-1}$ ,  $3 \times 10^{-26} \text{ cm}^3\text{s}^{-1}$ ,  $4 \times 10^{-26} \text{ cm}^3\text{s}^{-1}$  and  $5 \times 10^{-26} \text{ cm}^3\text{s}^{-1}$ . With the observed relic abundance value presented by the red dotted line, with accuracy band of  $3\sigma$ , from Planck collaboration [8].

In Fig. 5 we see that some of the plots intersects with the observed relic abundance value. This means that an average cross section of this value will create a correct relic abundance if the dark matter particles have the corresponding mass. For instance, if we study the green plot, where the average cross section is set to be  $3 \times 10^{-26} \text{ cm}^3\text{s}^{-1}$ , we see that it will create the correct relic abundance, compared to the observed value, if the dark matter particle mass is approximately 4 GeV. Similarly, we can see that if the dark matter mass is approximately between 40 GeV and 100 GeV, the average cross section that will give us the correct value for the relic abundance is approximately  $2 \times 10^{-26} \text{ cm}^3\text{s}^{-1}$ .

Even though these plots of the relic abundance give us a clue about what the average cross section has to be to get the observed value of the relic abundance, at the order of  $\sim 10^{-26}$ , it can be quite comprehensive to get exact results using this program. Fortunately, DarkSUSY has other programs that can do these calculations more precise.

#### 4.4.3 Calculations of average annihilation cross section

By the use of the `oh2_generic_wimp` example module in DarkSUSY, one can predict possible average cross sections,  $\langle\sigma v\rangle$ , that corresponds to current observations of the relic abundance,  $\Omega_\chi h^2$ . We use the observed value for the relic

abundance from the Planck collaboration [8],  $\Omega_\chi h^2 = 0.11933 \pm 0.00091$ . We assume the dark matter particles annihilates to SM particles, and we show the cases of annihilation to  $\bar{\nu}_e \nu_e$ ,  $\mu^+ \mu^-$ ,  $W^+ W^-$  and  $\bar{t} t$ .

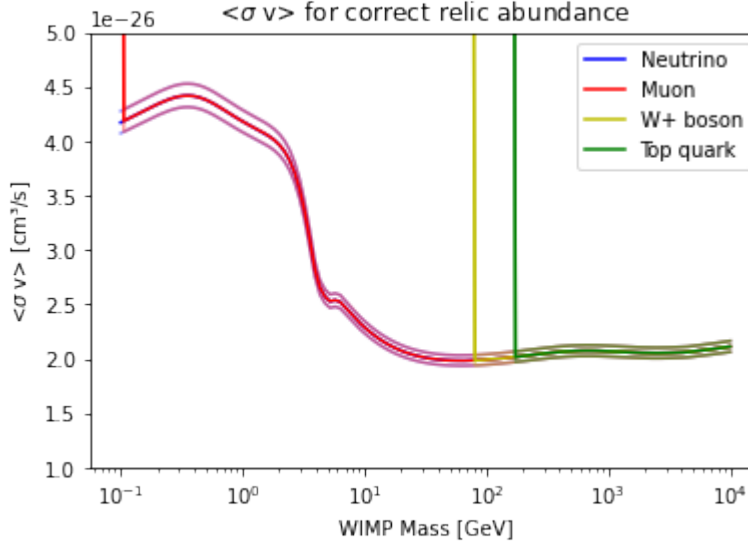


Figure 6: Average of annihilation cross section multiplied with velocity,  $\langle \sigma v \rangle$ , of the generic WIMP as a function of its mass,  $m_\chi$ , for the observed relic abundance [1]. The plot includes the particle coupling to SM particles  $\bar{t} t$ ,  $\bar{\nu}_e \nu_e$ ,  $\mu^+ \mu^-$  and  $W^+ W^-$ . Shown with accuracy of  $3\sigma$ , with the value of  $\sigma$  determined by the Planck collaboration [8].

Fig. 6 shows us  $\langle \sigma v \rangle$  of the annihilation from dark matter particles to specific SM particles, that gives the correct relic abundance for each different SM particle. As explained in [5], the generic WIMP module will not allow off-shell final state particles, which leads to the cross-section sharply dropping to zero for dark matter masses below the kinematic threshold [5]. This will further lead to a rapid decrease in the relic density from the specific annihilation, which explains the vertical lines in Fig. 6 [5]. We see that except for the vertical lines in the figure, the average cross section for different final state particles do not deviate much from the others. This tells us that  $\langle \sigma v \rangle$  for different final state particles do not depend on the mass of the SM particles, which is in agreement with the expression for relic abundance we derived, equation (52).

If we compare this plot with Fig. 5, we can see that for dark matter mass around 100 GeV, the average cross section that will give us the correct value for the relic abundance is approximately  $2 \times 10^{-26} \text{ cm}^3 \text{ s}^{-1}$ . This is the same result

as we arrived at from Fig. 5. Thus, we can see that these plots give the same results for the average cross section corresponding to mass and relic abundance, but the latter plot will show it in a clearer way.

#### 4.4.4 Calculations of freeze out $x$

By the use of the `generic_wimp` module, we can also calculate the value of  $x$  when the freeze out happens, and from this the freeze out temperature. We do this by modifying the example program `dsmain_wimp`, and inserting constant values for the average cross section. When using the values  $1 \times 10^{-25} \text{ cm}^3\text{s}^{-1}$ ,  $1 \times 10^{-26} \text{ cm}^3\text{s}^{-1}$ ,  $1 \times 10^{-27} \text{ cm}^3\text{s}^{-1}$ , and the annihilation channel for the neutrino, we get the result shown below.

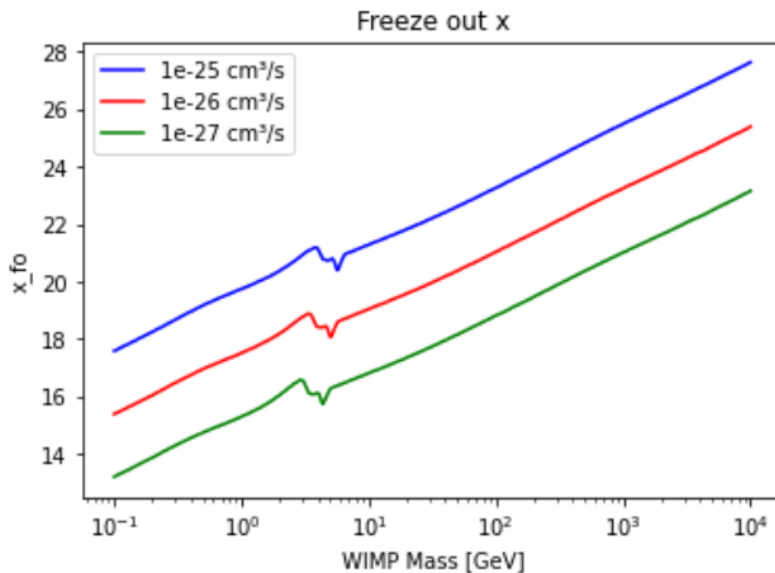


Figure 7: Freeze out  $x$  for corresponding WIMP mass, with neutrino as annihilation channel, for average cross section  $1 \times 10^{-25} \text{ cm}^3\text{s}^{-1}$ ,  $1 \times 10^{-26} \text{ cm}^3\text{s}^{-1}$ ,  $1 \times 10^{-27} \text{ cm}^3\text{s}^{-1}$ .

We see in Fig. 7, that the freeze out  $x$  increases logarithmically as the mass of the dark matter particles increases, except for at a section around dark matter particle mass from 25 GeV to 50 GeV. This bump corresponds to when the degrees of freedom changes rapidly.

Having obtained some values for  $x_{fo}$  with some corresponding values for the relic density,  $\Omega h^2$ , we can validate whether our derived formula for the relic abundance, equation (52), is approximately correct. We use the values for  $x_{fo}$

we got from DarkSUSY, and calculate the corresponding relic abundance,  $\Omega h^2$ . Then we compare our resulting value with the value DarkSUSY calculated for the same  $x_{fo}$ . To do our own calculations, we use the mathematical program Python.

To calculate an approximate relic abundance from a given freeze out  $x$ , we use our derived formula (52). Because DarkSUSY uses a constant average cross section,  $\langle\sigma v\rangle$ , when doing the calculations, we do as well. From this it follows that  $n = 0$ , so the expression remaining from equation (52) is

$$\Omega_\chi h^2 \simeq \left( \frac{45s_0}{2\sqrt{90}\pi \frac{\rho_c}{h^2}} \right) \frac{x_{fo}}{\langle\sigma v\rangle M_{Pl} \frac{g_{*s}}{\sqrt{g_*}}} \quad (53)$$

When calculating this, we need to determine a dark matter mass and an average cross section, and find the corresponding values of  $g_{*s}$  and  $g_*$ . We use reference [18] to find these values.

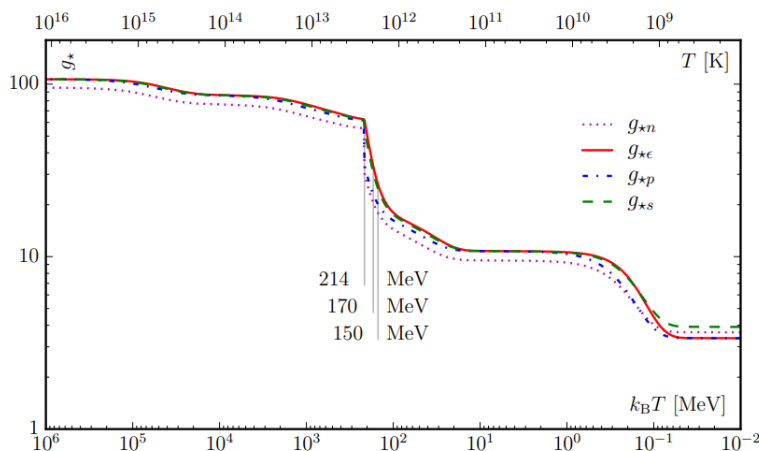


Figure 8: The evolution of the degrees of freedom of number density ( $g_{*n}$ ), energy density ( $g_{*e}$ , but we use notation  $g_*$ ), pressure ( $g_{*p}$ ), and entropy density ( $g_{*s}$ ) as functions of temperature. © CC BY 4.0, retrieved from reference [18].

Fig. 8 shows us that at most temperatures above  $T \simeq 10^{-1}$  MeV,  $g_{*s}$  and  $g_*$  are overlapping. Due to this, we set the approximation  $g_{*s} \simeq g_*$  for  $T > 10^{-1}$  MeV. To use this approximation, we have to make sure that we determine a dark matter mass and freeze out  $x$  that corresponds to a temperature higher than this.

With this in mind, we can choose the necessary properties to check the valida-

tion of our derived formula for the relic abundance. As we plotted values for  $x_{fo}$  for three different average cross sections, we want to check the freeze out  $x$  and corresponding relic abundance for each of the different average cross sections. Thus, we set  $\langle\sigma v\rangle$  to be  $10^{-25} \text{ cm}^3\text{s}^{-1}$ ,  $10^{-26} \text{ cm}^3\text{s}^{-1}$  and  $10^{-27} \text{ cm}^3\text{s}^{-1}$ .

We have to use an exact DM mass that DarkSUSY has used in its calculations, and we try for dark matter mass equal to 100 GeV. For this mass and average cross section  $10^{-25} \text{ cm}^3\text{s}^{-1}$ , DarkSUSY calculates  $x_{fo} = 23.265590333077910$ , which correponds to temperature

$$T = \frac{m_\chi}{x_{fo}} = \frac{100\text{GeV}}{23.265590333077910} \approx 4.29819\text{GeV} \quad (54)$$

We find the corresponding degrees of freedom for this temperature in *table A1* in the appendix of reference [18]. We approximate the temperature to be 5 GeV, the closest value in the table, and read from the table that the degrees of freedom are approximately  $g_{*s} \approx g_* \approx 85.50$  for this temperature. From the choice of these properties, the expected value for  $\Omega h^2$ , that DarkSUSY has calculated, is  $\sim 0.0255983$ .

$\Omega h^2$  is a dimensionless property, so we want to make sure that all units in the expression (53) cancels each other.  $x_{fo}$ ,  $g_{*s}$  and  $g_*$  are dimensionless, while  $s_0$ ,  $\rho_c$ ,  $M_{Pl}$  and  $\langle\sigma v\rangle$  have different units. When expressing (53) with units, and our chosen properties, we get

$$\Omega_\chi h^2 \simeq \left( \frac{45 \times 3000 \text{ cm}^{-3}}{2\sqrt{90} \pi 1.05 \times 10^4 \text{ cm}^{-3} \text{ eV}} \right) \frac{23.265590333077910}{10^{-25} \text{ cm}^3\text{s}^{-1} 2.4 \times 10^{18} \text{ GeV} \sqrt{85.50}} \quad (55)$$

$$\Omega_\chi h^2 \simeq 0.2157 \times 10^9 \text{ GeV}^{-1} \frac{23.265590333077910}{10^{-25} \text{ cm}^3\text{s}^{-1} 2.4 \times 10^{18} \text{ GeV} \sqrt{85.50}} \quad (56)$$

We can see that not all units cancel each other in the equation, so we need to find a relation between  $\text{cm}^3\text{s}^{-1}$  and eV to be able to do so. From the main assumption of our cosmological calculations,  $c = \hbar = k_B = 1$ , we can find such a relation. We use these units to find a relation by the use of  $[\hbar] = [\text{eV s}]$  and  $[c] = [\text{m/s}]$ .

$$\begin{aligned} \hbar &= 6.58 \times 10^{-16} \text{ eV s} = 1 \\ c &= 2.998 \times 10^8 \text{ m/s} = 1 \end{aligned}$$

(57)

Which can be rewritten, giving the expressions

$$1 \text{ m} = \frac{1 \text{ s}}{2.998 \times 10^8}$$

$$1 \text{ s} = \frac{1}{6.58 \times 10^{-16} \text{ eV}}$$

From this we can express

$$1 \text{ m} = \frac{1}{2.998 \times 10^8 \cdot 6.58 \times 10^{-16} \text{ eV}}$$

$$1 \text{ m} = \frac{1}{2.998 \times 6.58 \times 10^{-8} \text{ eV}}$$

And then we can express  $\text{cm}^3/\text{s}$  in terms of eV, and later cancel the units in our expression for the relic abundance.

$$\begin{aligned} \text{cm}^3/\text{s} &= \text{cm}^2 \cdot 10^{-2} \text{m}/\text{s} \\ \text{cm}^3/\text{s} &= \text{cm}^2 \cdot 10^{-2} \frac{1}{2.998 \times 10^8} \\ \text{cm}^3/\text{s} &= (10^{-2} \text{m})^2 \cdot 10^{-2} \frac{1}{2.998 \times 10^8} \\ \text{cm}^3/\text{s} &= \left( \frac{10^{-2}}{2.998 \times 6.58 \times 10^{-8} \times 10^{-9} \text{ GeV}} \right)^2 \frac{10^{-2}}{2.998 \times 10^8} \\ \text{cm}^3/\text{s} &= \frac{10^{-4}}{2.998^2 \times 6.58^2 \times 10^{-34} \text{ GeV}^2} \frac{1}{2.998 \times 10^{10}} \\ \text{cm}^3/\text{s} &\approx \frac{2.5697 \times 10^{27}}{2.998 \times 10^{10}} \text{ GeV}^{-2} \\ \text{cm}^3/\text{s} &\approx 8.57143 \times 10^{16} \text{ GeV}^{-2} \end{aligned} \tag{58}$$

We can insert this value for  $\text{cm}^3/\text{s}$  in the average cross section  $10^{-25} \text{ cm}^3/\text{s}$ . Then we change its units to  $\text{eV}^{-2}$ , and can get a dimensionless value for the



relic abundance.

$$\Omega_\chi h^2 \simeq 0.2157 \times 10^9 \text{ GeV}^{-1} \frac{23.265590333077910}{10^{-25} \times 8.57143 \times 10^{16} \text{ GeV}^{-2} 2.4 \times 10^{18} \text{ GeV} \sqrt{85.50}}$$

$$\Omega_\chi h^2 \simeq 0.026382280159656726 \quad (59)$$

We get (59) as our calculated value for the relic abundance.

We want to do this for all the different average cross sections, to validate the formula further. We vary the DM mass too, which gives us different properties for  $x_{fo}$ ,  $T$  and degrees of freedom. The results are presented in the table below.

Annihilation rate [cm <sup>2</sup> s <sup>-1</sup> ]	DM mass [GeV]	$x_{fo}$	Corresponding temperature [GeV]	Degrees of freedom, g <sub>*</sub>	Expected value of $\Omega h^2$ from DarkSUSY	Calculated value of $\Omega h^2$ from (53)
1x10 <sup>-25</sup>	100	23.265590333	4.29819	85.50	0.0255983	0.0263823
1x10 <sup>-26</sup>	1000	23.245025127	43.0199578	97.40	0.2392734	0.24696298
1x10 <sup>-27</sup>	501.187	20.369137183	24.61	88.45	2.1434394	2.2709367

Figure 9: Calculated properties for  $\Omega h^2$  with different values for chosen average cross section. The table lists average cross section, DM mass, freeze out  $x$ , corresponding temperature, corresponding degrees of freedom, and eventually the relic abundance calculated by both DarkSUSY and our calculations.

We can see in Fig. 9 that the calculated value of  $\Omega h^2$  in DarkSUSY is not exactly similar to the value we calculated by the use of equation (53). However, since the derived formula we have used to calculate the relic abundance is an approximation, we can accept that the obtained value compared to the expected value, has a small difference. The two values we compare are always of the same order, hence the formula we have derived can indeed be used, more or less, as a good approximation to calculate the expected relic abundance for certain values.

#### 4.4.5 Calculations of the yield

The yield is a very convenient way of measuring changes in density, for interactions on dark matter. By plotting the yield, we get a good illustration of the particles in DM acts before, and after the thermal freeze out. By the use of the example programs `dsmain_wimp` and `dsrdeqn`, we have plotted the yield against  $x$ , for different  $\langle\sigma v\rangle$ .

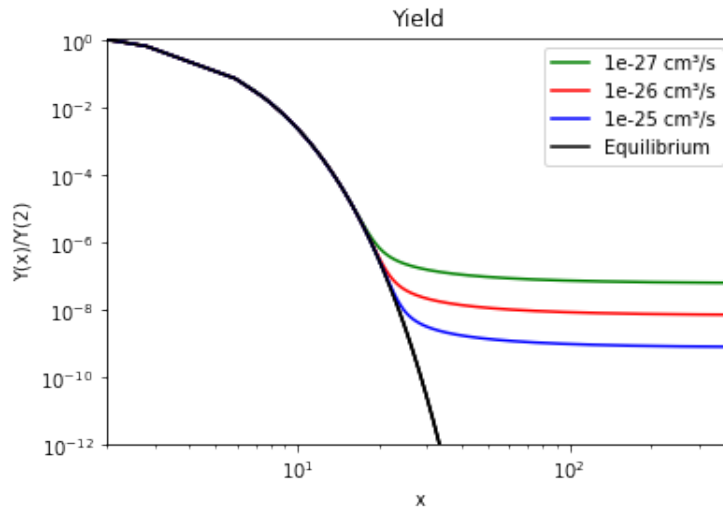


Figure 10: The yield as a function of  $x$ , for different average cross section  $1 \times 10^{-25} \text{ cm}^3\text{s}^{-1}$ ,  $1 \times 10^{-26} \text{ cm}^3\text{s}^{-1}$  and  $1 \times 10^{-27} \text{ cm}^3\text{s}^{-1}$ .

Fig. 10 shows us that the yield of all the different  $\langle\sigma v\rangle$  follow the value for the equilibrium yield, until the dark matter freezes out. The x-axis represents the  $x$ , and we see that for different  $\langle\sigma v\rangle$ , we have different freeze out  $x$ ,  $x_{fo}$ . However, we can see that the value for  $x_{fo}$  is approximately around  $x_{fo} \sim 20$  for all the average cross sections. The plot also shows us how the yield stays approximately constant after the thermal freeze out.

#### 4.5 The WIMP miracle

From the properties we have both derived and calculated, we learned that the average cross section of the interactions before thermal freeze out, should be of order  $\langle\sigma v\rangle \sim 10^{-26} \text{ cm}^3\text{s}^{-1}$ . Since the velocity of DM particles is non-relativistic, we assume the particles have velocity of  $v \ll c$ . We can specifically assume that the particles have average velocity of  $v \sim 0.1c$ .

We can then calculate the cross section,  $\sigma$  by

$$\sigma = \frac{\langle\sigma v\rangle}{0.1c} \approx \frac{10^{-26} \text{ cm}^3\text{s}^{-1}}{0.1 \times 3 \times 10^8 \times 100 \text{ cm s}^{-1}} \sim 10^{-36} \text{ cm}^2 \quad (60)$$

This value is in agreement with the fact that the particles is weakly interacting. The weakly interacting massive particle (WIMP) has been looked at as the best candidate for DM for a while. It has been thoroughly studied and searched for,

but has not been discovered yet [1]. The existence of a WIMP would solve many DM related problems.

The theory of supersymmetry predicts the existence of a WIMP, and this is why supersymmetry has been a popular theory to help with the explanation of the nature of DM for some time. The new superparticles proposed by the theory, have been calculated to have large masses, and will make good dark matter candidates. The lightest supersymmetric particle (LSP) is stable and will not decay into other particles, which means that it could have existed from the early Universe, as dark matter has. The LSP has therefore been viewed as a good candidate for dark matter due to its appropriate properties, and the LSP can either be the superparticle sneutrino, gravitino or the most favoured one, the neutralino. By the use of the properties of the LSP, one can calculate the amount of DM that would be produced if this were the correct particle model. The resulting amount from the calculation is very close to the observed amount of dark matter, and many do not think that this is a coincident. Physicists refer to this as the *WIMP miracle*. [19] [20]

A generic WIMP is also favoured as a DM candidate because it should in principle be easy to detect. It has been thoroughly searched for in both direct detection experiments, indirect detection, and collider searches. We will look more into this in section 6, but will firstly look into a specific example of the WIMP.

## 5 Scalar singlet

When assuming the freeze out to be the production mechanism of DM, we discovered that a good candidate for the DM particle, is a WIMP that can annihilate into SM particles. We want to look at a simple model of a WIMP as the DM candidate, with few necessary parameters.

Even though the theory of supersymmetry and the LSP has been a favoured DM candidate, this particle model is a bit too complicated to be able to calculate wanted DM properties precisely. We want to find models that are simple enough to do calculations, and at the same time consistent with previous evidence of dark matter. In this section we will look into the simplest extension of the SM, the scalar singlet. [4]

The simplest possible extension of the Standard Model is the addition of a singlet scalar field,  $S$ . This model of a scalar singlet has been proposed as a particle model for a non-baryonic DM particle [4]. The scalar singlet particle is characterized by only three parameters, making it simple enough to do calculations of the DM properties. At the same time, the model is still complicated enough to give interesting results of the calculations.

The scalar singlet is a spinless particle, electrical neutral, and stable. When working with scalar singlet dark matter, we assume that the dark matter consists of only this single species of particles. The three parameters characterizing the scalar singlet is the particle mass,  $m_S$ , the particles self-coupling,  $\lambda_S$ , and the particle coupling to the Higgs boson,  $\lambda$ . The mass of the scalar singlet,  $m_S$ , is believed to be between 10-100 GeV, such that the DM is cold. The self-coupling of the scalar singlet,  $\lambda_S$ , is constrained due to the observations of the Bullet cluster in 2006 [3]. Therefore,  $\lambda_S$  need to be small enough such that it corresponds to these observations. The most important coupling to study is the coupling with the Higgs boson,  $\lambda$ . When looking into the Higgs portal coupling to SM particles, this is also closely related to the expected cross section,  $\sigma \propto \lambda^2$ . [4]

When using the scalar singlet model, we have to consider some constraints to make the model work. The constraint for these couplings, is that we have vacuum stability, and that we have a desirable symmetry-breaking pattern. We want the scalar potential to spontaneously break the electroweak symmetry, but not to break the symmetry  $S = -S$ . After the electroweak symmetry breaks, the scalar potential responsible for the interactions with  $S$ , takes the form

$$V = \frac{1}{2}\mu^2 S^2 + \frac{1}{2}\lambda S^2 H^\dagger H, \quad (61)$$

where  $H^\dagger H = \frac{1}{2}(h + v_0)^2 = \frac{1}{2}(h^2 + 2hv_0 + v_0^2)$ . Then we can rewrite (61) to

$$V = \frac{1}{2}\mu^2 S^2 + \frac{1}{4}\lambda v_0^2 S^2 + \frac{1}{4}\lambda h S^2 + \frac{1}{2}\lambda v_0 h^2 S^2. \quad (62)$$

$\mu$  is a mass parameter,  $v_0 = 246$  GeV is the Higgs vacuum expectation value (VEV), and  $h$  is the Higgs boson [4]. The first two terms in the potential (62) represents the mass of the scalar singlet, where

$$\begin{aligned} V \ni \frac{1}{2}m_S^2 S^2 &= \frac{1}{2}\mu^2 S^2 + \frac{1}{4}\lambda v_0^2 S^2 \\ \Rightarrow m_S &= \sqrt{\mu^2 + \frac{1}{2}\lambda v_0^2} \end{aligned} \quad (63)$$

Furthermore, the two last terms in (62) represents the possible couplings to  $S$ , with couplings  $hS^2$  and  $h^2S^2$ . This allows for the following annihilation to occur.

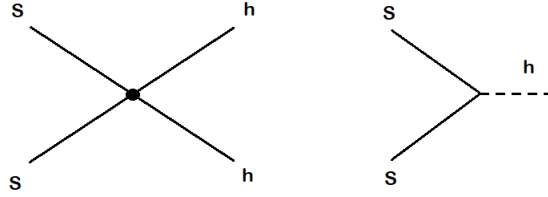


Figure 11: Feynman diagram of possible annihilation. On the right-hand side the coupling  $h^2S^2$ . On the left-hand side the coupling  $hS^2$ .

The Higgs exchange is shown on the right-hand side of Fig. 11. Through the Higgs exchange,  $S$  can interact with different SM particles as shown below.

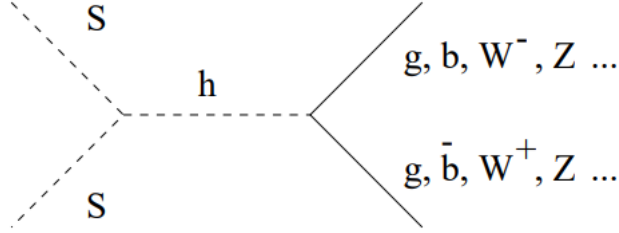


Figure 12: Feynman diagram of annihilation of the scalar singlet particle via Higgs exchange. The s-channel annihilation. We can see the different annihilation channels, and these will be allowed depending on the value of  $2m_S$ . Copyright © 2001 Published by Elsevier B.V.. Retrieved from [4] with permission.

## 5.1 DarkSUSY results

In this section we want to use DarkSUSY to do some specific calculations of the properties of the scalar singlet DM.

### 5.1.1 Silveira-Zee module

The Silveira-Zee module is the module in DarkSUSY that is made for calculations of the scalar singlet particle model. The module uses the mass of the scalar singlet boson,  $m_S$ , and its coupling to the Higgs boson,  $\lambda$ , as parameters. By inserting values for these parameters, the program can do calculations of the relic abundance and average cross section of the particles at thermal freeze out. [5]

### 5.1.2 Calculations of relic abundance

The relic abundance of the scalar singlet DM is mostly determined by the s-channel annihilation by Higgs exchange,  $SS \rightarrow X$ , where  $X$  is a pair of SM particle-antiparticle, for instance  $\pi\pi$ ,  $\mu^+\mu^-$  etc. [4].

By the use of the observed value for the relic abundance of DM,  $\Omega_S h^2 \approx 0.11933$  [8], we can use the `silveira.zee` module in DarkSUSY to produce a plot of the relation between  $\lambda$  and  $m_S$  for the wanted relic abundance. We do this by modifying the `oh2_ScalarSinglet` program.

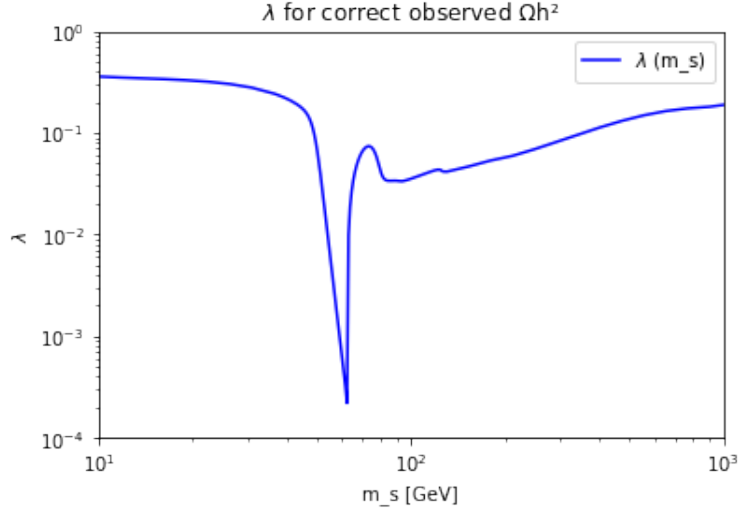


Figure 13: The Higgs coupling,  $\lambda$ , corresponding to different mass,  $m_S$ , for the observed value of the relic abundance,  $\Omega h^2 \approx 0.11933$ .

Fig. 13 shows us that for this variety of scalar particle mass, the Higgs coupling,  $\lambda$ , mostly take the value between the order of  $\sim 10^{-1}$  and  $\sim 10^{-3}$ .

As previously derived in section 4.3, equation (52) gives us the approximate relic abundance for specific freeze out  $x$ ,  $x_{fo}$ , and average cross section,  $\langle\sigma v\rangle$ . The average cross section for the scalar singlet is determined by the Higgs coupling,  $\lambda$ , and the mass of the particle,  $m_S$ . Hence, the relic abundance is dependent on these parameters as well. For most values of  $m_S$ , equation (52) explains the curve in our plot. However, there are certain exceptions to this. The Higgs threshold, that is if  $m_S \approx 1/2m_h$ , is an example of a case where the equation is not accurate enough. This is noticeable in our plot, where the drop in the curve is for this threshold,  $m_S = 1/2m_h$ , and  $m_h \approx 126$  Gev [12].

The average cross section's dependence of  $\lambda$  and  $m_S$ , for the limits when  $m_S$  is very large or very small, can be expressed by

$$\sigma v \propto \frac{\lambda^2 m_S^2}{m_h^4} \quad , \quad \text{if } m_S \ll m_h \quad (64)$$

$$\sigma v \approx \frac{\lambda^2}{4\pi m_S^2} \quad , \quad \text{if } m_S \gg m_h \quad (65)$$

which is retrieved from [4]. Since we already have seen that  $x_{fo} \sim 20$  for the range of cross sections and masses we use in our model, we can look at  $x_{fo}$  as constant. Due to this, to get the correct relic abundance, equation (52) shows

us that  $\langle\sigma v\rangle$  also need to be held constant, while  $\lambda$  and  $m_S$  can vary, provided  $g_*$  is also held constant. This is called the abundance constraint.

If  $m_S$  is very small,  $\lambda$  increases as  $m_S$  decreases. If  $m_S$  is very large,  $\lambda$  will increase with increasing  $m_S$ . This is shown in the two equations above. [4]

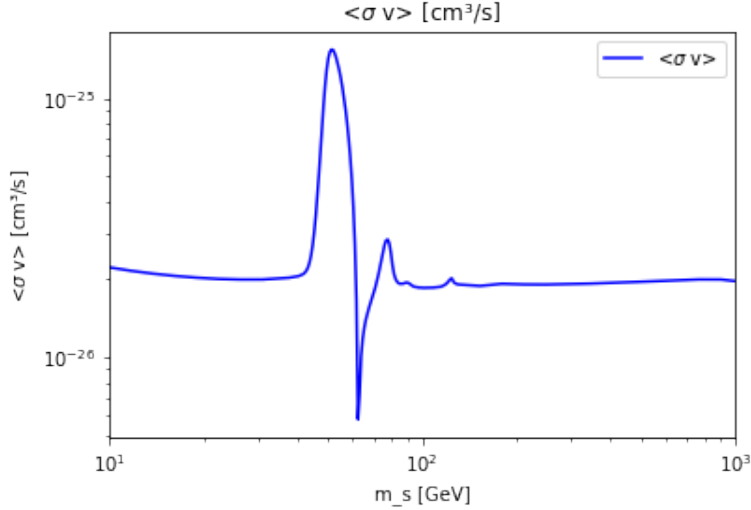


Figure 14: Correct average cross section for the observed relic abundance of DM. The average cross section can be seen as approximately constant for small and large  $m_S$ . The region where  $m_S \approx 1/2m_h$ , shows us how the average cross section will vary around the Higgs threshold.

The relic abundance constraint is shown in Fig. 14. To get the correct relic abundance, with approximately constant freeze out  $x$ , the average cross section is approximately constant for small and large  $m_S$ , as in Fig. 14. However, similar to Fig. 13, the Higgs threshold is an exception. At  $m_S \approx 1/2m_h$  our curve makes a jump, which tells us that equation (52) will not be a good approximation in this region, and this impacts the average cross section. Fig. 14 is also consistent with our previous calculations, where we found that the average cross section of the DM particles is of order  $\sim 10^{-26} \text{ cm}^3\text{s}^{-1}$ .



## 6 Experimental detection of dark matter

From the properties we have both derived and calculated, we learned that the average cross section of the interactions before thermal freeze out should be of order  $\langle\sigma v\rangle \sim 10^{-26} \text{ cm}^3\text{s}^{-1}$ , and a cross section of order of  $\sigma \sim 10^{-36} \text{ cm}^2$ . Based on this order of cross section, one should in theory be able to detect WIMP particles in different experiments, if this is the correct particle model. DM particles is actively searched for, by many different types of experiments. We will now look into experiments searching for DM particles by indirect detection, collider searches and direct detection.

### 6.1 Indirect detection

Experiments trying to detect DM particles by indirect detection, want to detect SM particles that have been produced by the annihilation of two DM particles in the Universe, or from a decaying DM particle. Indirect detection experiments can be done differently, depending on which particle they are trying to detect. A popular particle to try to detect is the photon. This is because it is easily detected, and their propagation through the Universe is almost unaffected by intergalactic and interstellar media. Charged particles are also quite easy to detect, but their propagation through space is highly affected by magnetic fields. Their propagation is thus quite hard to model. As for neutrinos, their propagation is also basically unaffected through the Universe, but these particles are on the other hand much harder to detect. [1]

Independent of the difficulty of their detection, one has bigger chance to detect the particles produced in the denser regions of DM in the Universe. There are three different galactic density profiles: the NFW (Navarro-Frenk-White) profile, Einasto profile, and the Burkert profile. These profiles measure the distribution of density in galaxies. Even though these profiles are not necessarily too different from each other, the fact that different density profiles of galaxies are possible, shows us that there can be large uncertainties in the measurements. This makes the indirect detection of DM, and the search for the SM particles, more complicated. [1]

Considering our earlier calculations of the particle cross section, this experiment should be able to detect DM particles indirectly by the produced SM particles. This, however, is not the case, and there has not been detected any SM particles that could indicate the existence of DM. This can be both due to large uncertainties in measurements, but could also be an indication that our earlier derivations and assumptions are incorrect.

## 6.2 Collider searches

Colliders are accelerators that send particles with equal mass and kinetic energy towards each other with significantly high velocities [9]. When the particles collide, in a high energy collision, they create a reaction where new particles are formed.

In the searches for DM particles, by the use of colliders, one sends two SM particles in a high energy collision, with the hope that the collision will produce new physics particles, or generating heavy particles that can decay into new physics particles. Even though most of SM particles have very constrained decays, some of them still have smaller constraints on their decay. In this case, the Higgs boson is interesting. The decay width of the Higgs boson, meaning probability of a certain decay channel to happen, can be up to 26% for the decay into invisible particles [1]. The Higgs boson can then have couplings to invisible particles with mass below 60 GeV. [1]

There are different types of colliders, for instance hadron colliders and lepton colliders. The Large Hadron collider (LHC) is, as the name indicates, a collider for hadrons. It has a high luminosity, making it suitable in the probe of small couplings, and strong interactions. Lepton colliders are well suited to study the electroweak sector of the SM. These colliders have a lower luminosity, giving it a more limited reach. However, this makes it more precise in its measurements. Both hadron and lepton colliders are used in the search for DM particles in colliders, but due to the DM particles characteristics to be weakly interacting and neutral, the particles will only have small Higgs couplings to the quantum chromodynamic sector of the SM. To detect these small couplings, hadron colliders are suited best, for instance the LHC.

When using these colliders, one looks at the energy conservation of high energy reactions before and after the collision. Some reactions have missing transverse energy in the final state. This missing energy is thought to be the indication that new heavy particles is made, and that these particles can decay into DM particles. For this theory to be true, one relies on the characteristics of new physics to be true, and the existence of heavier unknown particles. [1]

If DM particles really are produced in a collider, one would not have been able to detect them due to their weak interactions. To figure out whether the particles have been made, one has to look at the other particles that has been made in the process as well, and the conservation of momentum. For instance, in the LHC the missing transverse energy, referring to the DM particles, would be accompanied by a high energy jet (spray of particles). In lepton colliders, the accompanying particle should be a hard photon. The annihilation channels

studied with these results are called *mono-X*, where identical particles are colliding. The X-particles in these cases can be a jet, photon, top quark, gauge boson, a Higgs boson, or a lepton. [1]

However, there has been no such discoveries in collider searches yet. This could be because it is quite hard to relate the missing energy in a reaction to DM particles, or that our particle model simply is the wrong particle model.

### 6.3 Direct detection

By the assumption that DM particles have an approximate mass of 100 GeV, and the fact that we know that the local DM density in the Milky Way is of the order of  $0.4 \text{ GeV/cm}^3$ , we can calculate that there should be approximately 4000 DM particles in each cubic meter of the galaxy at all times. When considering that galactic halos are fixed compared to rotations of the galaxy, DM has a relative velocity of 200 km/s. If these values are approximately correct, there should travel about  $\sim 10^{16}$  DM particles through each cubic meter in the galaxy, during the period of one year. [1]

If this is actually the case, there should be  $\sim 10^{16}$  DM particles travelling through every cubic meter here on Earth in a year as well, and we should be able to detect some of these particles. This would be direct detection of the DM particles. Due to the DM particles interaction with nucleons, one should be able to measure the nucleon's recoil energy after the interaction with DM. From this we also want to be able to determine the DM particle mass, and cross section with the nucleons.

#### 6.3.1 Constraints of dark matter

By assuming specific DM particle masses and trying to detect the particles interaction with the nucleons, one can confirm or decline whether particles of this mass are travelling past the Earth. By doing this for several different masses of DM, this can be used to set constraints of the DM mass, and nature of DM particles. There have been many experiments trying to directly detect the DM particles by this setup. An overview of the constraints that has been found from the experiments CDMSLite [21], PANDAX-II [22] and XENON1T [23] can be viewed below in Fig. 15.

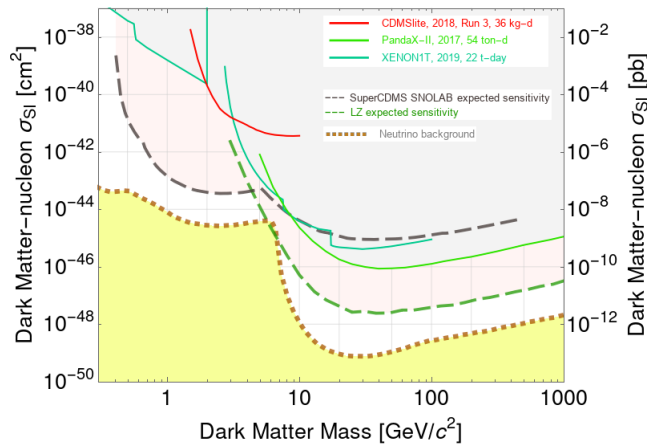


Figure 15: Constraints of scattering cross sections and DM mass for DM particles, from dark matter detection experiments CDMSlite [21], PANDAX-II [22] and XENON1T [23]. Solid lines represent the constraints that already have been found, while the dashed lines represent future experiments (as of 2021) [1]. The yellow regions represents the cosmic neutrino background [1]. © 2021 Elsevier B.V. All rights reserved. Retrieved from [1], with permission.

### 6.3.2 Constraints of scalar singlet dark matter

The XENON detector is a device trying to detect DM particles by their interactions with xenon. The detector is a two-phase time projection chambers (TPC), and it holds a large volume of pure liquid xenon to act as a WIMP target. The detection of ionized xenon due to the nuclear recoils of WIMPs off the xenon nuclei, or emitted xenon scintillation light, would be an indication of the existence of DM. To get the limits for the DM properties, it is assumed in [24] that the DM particle has spin-independent interactions with WIMP nuclei, which can correspond to the scalar singlet,  $S$ , with spin 0. [24] [25]

The XENON10 experiment, operated in 2007, managed to get the best constraints of the DM particles seen at the time [24]. The constraints were set because the experiment should be able to detect DM particles, if the particles had the corresponding cross section and mass. However, when no such particles were detected, it told us that the DM particles would not have these properties when using the scalar singlet particle model.

To be able to detect lower nucleon scattering cross section and lower coupling, one increased the mass of the TPC by a factor of 10 and decreased the electromagnetic background by a factor of 100 [25]. This experiment, called XENON100, was also successful, and achieved even more precise con-

straints of the DM WIMP. Going forward from this, the following experiments were performed for lower and lower cross sections and coupling, with increasingly larger mass of the TPC. These experiments were called XENON100x5, XENON100x20, XENON1T etc. None of these experiments were able to detect any particles, and the constraints of the particle has become more and more stringent. XENON1T is the experiment which has achieved the most precise constraints of the DM particle as of today. [24]

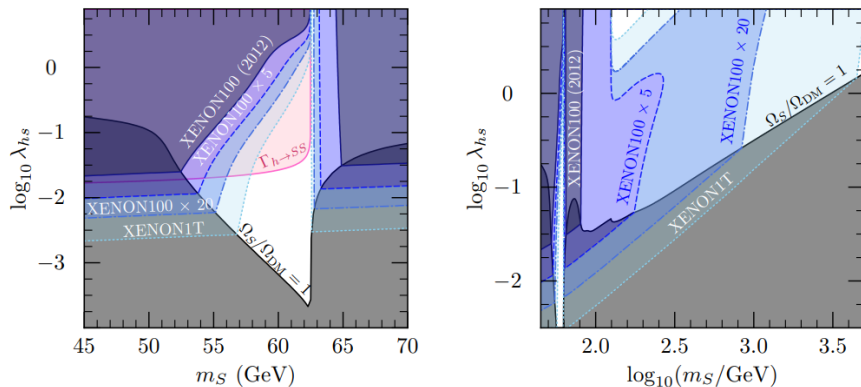


Figure 16: Constraints of scalar singlet dark matter, obtained from direct detection experiments, assuming the scalar singlet is the dominant particle in DM. The shaded and colored areas is the excluded properties of  $\lambda$  and  $m_S$ , which the particles cannot have. In this figure,  $\lambda_{hs}$  corresponds to what we denote as  $\lambda$  in this thesis. Different experiments are written in certain areas to show which constraint that has been obtained from which experiment. At the left-hand side there is a close-up of the correct relic abundance region. At the right-hand side, the full mass range is shown. © 2013 American Physical Society. Retrieved from [24], with permission.

In Fig. 16, we can see all the constraints of the coupling and DM particle mass that has been detected by the different XENON experiments. We see that most of the figure is shaded by some color, which means that the DM particle cannot have this corresponding mass and coupling. This means that by the use of the scalar singlet particle model with freeze out as production mechanism, the DM particle has quite limited values it can take.

When looking at these three types of experiments and the fact that none of them have been able to detect DM particles yet, one can question whether our previous predictions and calculations of DM particles average cross section etc. is correct. If this is incorrect, it would mean that the production model of the thermal freeze out is also incorrect. All the constraints found by the direct de-

tection experiments of scalar singlet, tells us that it is quite improbable to find DM particles corresponding to this particle model. In the next section, section 7, we will briefly look into a second possible production model, and study the properties of DM in this case.

## 7 Freeze in of scalar singlet DM

The WIMP is the most studied particle model for a DM candidate, because it is a simple particle that can acquire the correct relic abundance with freeze out as the production mechanism. As the WIMPs have yet to be experimental detected, we must consider the possibility that this is not the correct model for DM.

An alternative to the WIMP model, is the FIMP model. FIMP is short for feebly interacting massive particle, and is a particle model with significantly smaller Higgs coupling than the WIMP [26]. Both WIMPs and FIMPs can satisfy the constraints of DM in the scalar singlet model, only for the FIMP model, a new production mechanism of DM has to be introduced. When looking into this new production mechanism, we will still assume the scalar singlet particle model.

The *freeze in* is a production mechanism of DM where the FIMPs never reach thermal equilibrium in the early Universe, and are slowly produced by particle collisions or decays in the thermal plasma [26]. The FIMPs are produced as the Universe expands and the temperature decreases. When the temperature becomes smaller than the DM mass, the plasma no longer has the energy to produce more particles [26]. At this temperature, the production of DM will stop, and the already produced DM will *freeze in*.

We can describe the freeze in process from our derived Boltzmann equation (41). For the freeze in mechanism, the yield of DM is very small,  $Y_\chi \ll Y_{\chi_{eq}}$ , and can be neglected. We are then left with

$$\frac{dY_\chi}{dx} = \frac{s\langle\sigma v\rangle}{Hx} Y_{\chi_{eq}}^2. \quad (66)$$

This show us that the yield will increase, due to the right-hand side of (66) being positive. It will increase until it freezes in, and then it will be approximately constant after this. Fig. 17 show us that this is the case.

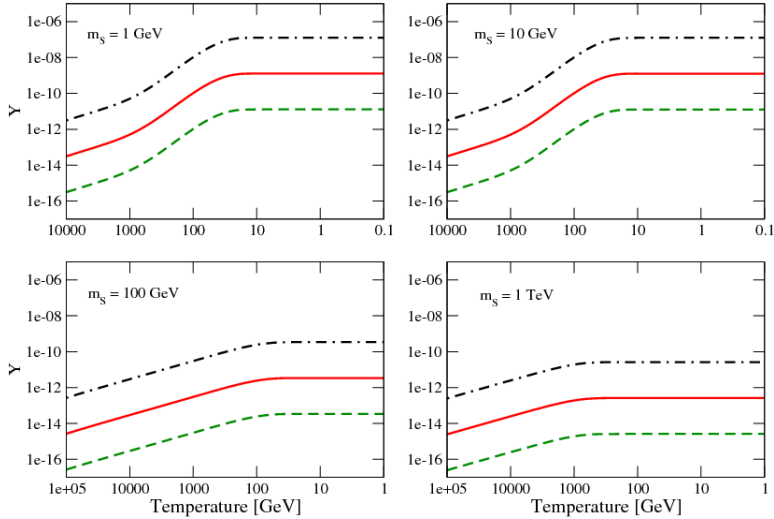


Figure 17: The yield as a function of temperature, for different  $\lambda$  and scalar singlet mass,  $m_S$ . The dash-dotted line represents  $\lambda = 10^{-10}$ , the solid line represents  $\lambda = 10^{-11}$ , and the dashed line represents  $\lambda = 10^{-12}$ . This result was obtained in 2011, before the Higgs mass was found, and the Higgs mass was in these plots set to be  $m_h = 120$  GeV. Copyright © 2011, SISSA, Trieste, Italy. Retrieved from [26], with permission.

Due to the weak interactions of the FIMPs, and that they are never abundant enough to annihilate themselves, there are two different processes that could create the feebly interacting DM particles. The DM particles could either be produced by the annihilation of two SM particles, or by the decay of a heavier FIMP. In the first case, we consider that the DM particles are produced by the  $2 \rightarrow 2$  processes,  $ab \rightarrow SS$ . In the second case, an example is the Higgs decay,  $h \rightarrow SS$ . However, when we assume the scalar singlet to be the FIMP, which is the heaviest FIMP in this model, only the first process will be relevant.

The weak interactions of the FIMPs also indicate small  $\lambda$ . If the relic abundance for the freeze in followed the same equation as the freeze out, (52), the relic abundance would have increased as  $\lambda$  decreased. This is due to the dependence of  $\lambda$  in  $\langle \sigma v \rangle$  for the scalar singlet, from equations (64) and (65). However, if  $\lambda = 0$ , there would have been no particle interactions in the early Universe to produce DM, and DM would never have been produced. So, eventually as  $\lambda$  decreases and approaches zero, the relic abundance must also decrease, until it vanishes for  $\lambda = 0$ . Due to the increase and eventually decrease in relic density, there must exist a smaller value of  $\lambda_{fimp}$  that corresponds to the observed relic abundance today. [26]



## 7.1 DarkSUSY results

By the use of DarkSUSY, and the `silveria_zee` module for the scalar singlet, we can produce a plot of the expected value of  $\lambda_{fimp}$  for the correct relic abundance.

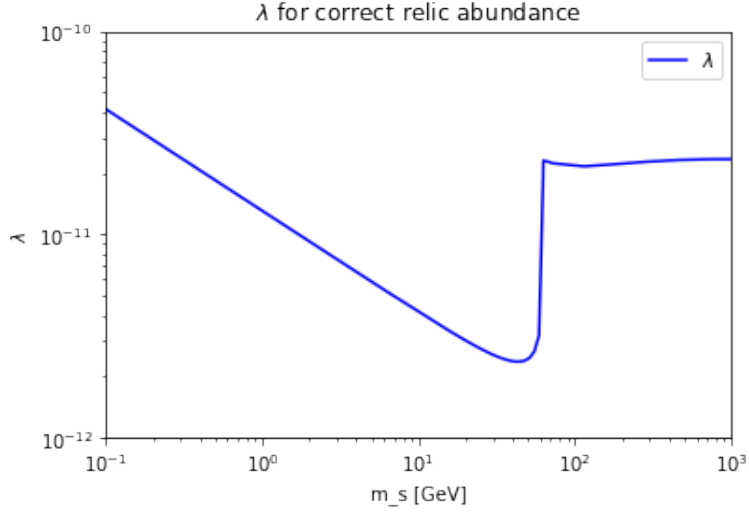


Figure 18: Expected value of  $\lambda$  corresponding to the singlet mass,  $m_S$ , for the correct relic abundance, with the freeze in as the production mechanism.

Fig. 18 shows us that for the FIMPs in the freeze in, the Higgs coupling has to be significantly smaller than for the WIMPs in the freeze out. In this case the coupling is of the order  $\lambda \sim 10^{-11} - 10^{-12}$ .

Despite this significant difference in the Higgs coupling,  $\lambda$ , both WIMPs and FIMPs would be able to create the DM abundance we observe today. WIMPs would be produced by the freeze out, and FIMPs by the freeze in. FIMPs is not experimental detectable like WIMPs due to its feeble coupling, and FIMPs is therefore a good candidate for DM particles, that can also explain the absence of experimental detection of the DM particles.

## 8 Conclusion

In this thesis we have looked at possible production mechanisms of dark matter, and especially at the freeze out mechanism.

To understand the aspects of dark matter and its production, we first went through some background theory. This was important for further understanding in the thesis. We went into how evidence for dark matter was discovered, and what we can know about the nature of DM from these observations.

When investigating the freeze out as a production mechanism, we derived and solved the Boltzmann equation analytically. From this we also derived an approximate formula for the relic abundance of DM. This was used to calculate expected relic abundance, for different properties of  $\langle\sigma v\rangle$  and freeze out  $x$ .

By the use of the Fortran-program DarkSUSY, we calculated the yield,  $\langle\sigma v\rangle$ , relic abundance and freeze out  $x$  of the DM, assuming the freeze out to be the production mechanism of DM. Our calculated relic abundance was compared to the calculations DarkSUSY made, and the observed value of DM abundance from the Planck collaboration [8]. From this we could see which of the corresponding values for yield,  $\langle\sigma v\rangle$  and freeze out  $x$  that would correspond to the observed properties of DM.

These calculations told us a lot about the characteristics of the DM particles, and we learn that the favoured DM candidate for this production mechanism is the WIMP. We look further into the WIMP miracle, and specific candidates to the WIMP. We focus especially on the simplest addition to SM, the scalar singlet. We also do some calculations of this specific WIMP candidate in DarkSUSY.

Based of the properties we found from our assumption of the freeze out production mechanism, and that the DM particle is a WIMP, detection experiments should be able to detect the DM particles. There are different ways to do so, and we look into the three most commonly used methods: direct detection, indirect detection and collider searches. These experiments have all been performed, but none of them have been able to detect any DM particles, or indications that such DM particles exist. The experiments still provide us with some constraints of the mass and coupling of the DM particles. However, with all the constraint that have been found, the probability that the freeze out mechanism is the correct production mechanism has become smaller and smaller.

By the results of the experiments, we have to consider a new production mechanism for DM. The mechanism of the freeze in has been proposed [26], and we look briefly into this. This production mechanism gives the correct relic abundance for DM, and by calculations in DarkSUSY we see that it gives the

correct  $\langle\sigma v\rangle$  as well. The difference of this production mechanism is that the particles that are produced will have to have even weaker interactions than the WIMPs, and are called feebly interacting massive particles (FIMPs). The weak interactions of these particles can also explain why the DM particles have not been detected by experiments.

The production mechanism freeze in, and the FIMP model, needs to be thoroughly studied as a DM production mechanism and candidate. This theory is an interesting theory that can explain DM thoroughly. Hopefully detection methods that can detect this type of particles are discovered in the coming decades, such that the freeze in theory of DM can be either confirmed or disproved. For further reading of the freeze in mechanism and the FIMP, please view reference [26] and [27].

## References

- [1] A. Arbey and F. Mahmoudi, "Dark matter and the early Universe: a review", *Prog. Part. Nucl. Phys.* **119**, 103865 (2021) doi:10.1016/j.pnnp.2021.103865 [arXiv:2104.11488 [hep-ph]].
- [2] R. H. Sanders, "Early history of the dark matter hypothesis", from *The dark matter problem: a historical perspective*. Cambridge: Cambridge University Press; 2010.
- [3] D. Clowe, M. Bradac, A. H. Gonzalez, M. Markevitch, S. W. Randall, C. Jones and D. Zaritsky, "A direct empirical proof of the existence of dark matter", *Astrophys. J. Lett.* **648**, L109-L113 (2006) doi:10.1086/508162 [arXiv:astro-ph/0608407 [astro-ph]].
- [4] C. P. Burgess, M. Pospelov and T. ter Veldhuis, "The Minimal model of nonbaryonic dark matter: A Singlet scalar", *Nucl. Phys. B* **619**, 709-728 (2001) doi:10.1016/S0550-3213(01)00513-2 [arXiv:hep-ph/0011335 [hep-ph]].
- [5] T. Bringmann, J. Edsjö, P. Gondolo, P. Ullio and L. Bergström, "DarkSUSY 6 : An Advanced Tool to Compute Dark Matter Properties Numerically", *JCAP* **07**, 033 (2018) doi:10.1088/1475-7516/2018/07/033 [arXiv:1802.03399 [hep-ph]].
- [6] P. A. Tipler, R. A. Llewellyn. *Modern physics*. 6th ed. New York: W.H. Freeman; 2012. XV, 702, 62.
- [7] E. W. Kolb, M. S. Turner, *The early universe*, Vol. 69, Cambridge, Mass: Perseus Publ; 1994. XLII, 547.
- [8] N. Aghanim *et al.* [Planck], "Planck 2018 results. VI. Cosmological parameters", *Astron. Astrophys.* **641**, A6 (2020) [erratum: *Astron. Astrophys.* **652**, C4 (2021)] doi:10.1051/0004-6361/201833910 [arXiv:1807.06209 [astro-ph.CO]].
- [9] R. A. Serway, C. J. Moses and C. A. Moyer, *Modern physics*, 3rd ed., Belmont, Calif: Thomson Brooks/Cole; 2005. XV, 600, 31.
- [10] P. A. Tipler, G. Mosca, *Physics for scientists and engineers*, 5th ed., extended. New York: Freeman; XXX, 1356, 107.
- [11] Retrieved from "File:Standard Model of Elementary Particles.svg", by MissMJ, 09.17.19, ([https://en.wikipedia.org/wiki/File:Standard\\_Model\\_of\\_Elementary\\_Particles.svg](https://en.wikipedia.org/wiki/File:Standard_Model_of_Elementary_Particles.svg)). CC Attribution 3.0 Unported license: (<https://creativecommons.org/licenses/by/3.0/deed.en>)

- [12] G. Aad *et al.* [ATLAS], "Observation of a new particle in the search for the Standard Model Higgs boson with the ATLAS detector at the LHC", *Phys. Lett. B* **716**, 1-29 (2012) doi:10.1016/j.physletb.2012.08.020 [arXiv:1207.7214 [hep-ex]].
- [13] G. Bertone, D. Hooper and J. Silk, "Particle dark matter: Evidence, candidates and constraints", *Phys. Rept.* **405**, 279-390 (2005) doi:10.1016/j.physrep.2004.08.031 [arXiv:hep-ph/0404175 [hep-ph]].
- [14] D. Merritt, "The Distribution of Dark Matter in the Coma Cluster", *The Astrophysical Journal*, vol. 313, p. 121, 1987. doi:10.1086/164953.
- [15] F. Zwicky, "Die Rotverschiebung von extragalaktischen Nebeln" [The red shift of extragalactic nebululae]. *Helvetica Physica Acta* (in German). 6: 110–127 (1933).
- [16] R. H. Sanders, "Direct evidence: extended rotation curves of spiral galaxies", from *The dark matter problem: a historical perspective*. Cambridge: Cambridge University Press; 2010.
- [17] V. C. Rubin and W. K. Ford, Jr., "Rotation of the Andromeda Nebula from a Spectroscopic Survey of Emission Regions", *Astrophys. J.* **159**, 379-403 (1970) doi:10.1086/150317
- [18] L. Husdal, "On Effective Degrees of Freedom in the Early Universe", *Galaxies* **4**, no.4, 78 (2016) doi:10.3390/galaxies4040078 [arXiv:1609.04979 [astro-ph.CO]].
- [19] J. Ellis and K. A. Olive, "Supersymmetric Dark Matter Candidates", [arXiv:1001.3651 [astro-ph.CO]].
- [20] S. Chang, R. Edezhath, J. Hutchinson and M. Luty, "Effective WIMPs", *Phys. Rev. D* **89**, no.1, 015011 (2014) doi:10.1103/PhysRevD.89.015011 [arXiv:1307.8120 [hep-ph]].
- [21] R. Agnese *et al.* [SuperCDMS], "Search for Low-Mass Dark Matter with CDMSlite Using a Profile Likelihood Fit", *Phys. Rev. D* **99**, no.6, 062001 (2019) doi:10.1103/PhysRevD.99.062001 [arXiv:1808.09098 [astro-ph.CO]].
- [22] X. Cui *et al.* [PandaX-II], "Dark Matter Results From 54-Ton-Day Exposure of PandaX-II Experiment", *Phys. Rev. Lett.* **119**, no.18, 181302 (2017) doi:10.1103/PhysRevLett.119.181302 [arXiv:1708.06917 [astro-ph.CO]].
- [23] E. Aprile *et al.* [XENON], "Light Dark Matter Search with Ionization Signals in XENON1T", *Phys. Rev. Lett.* **123**, no.25, 251801 (2019) doi:10.1103/PhysRevLett.123.251801 [arXiv:1907.11485 [hep-ex]].

- [24] J. M. Cline, K. Kainulainen, P. Scott and C. Weniger, "Update on scalar singlet dark matter", *Phys. Rev. D* **88**, 055025 (2013) [erratum: *Phys. Rev. D* **92**, no.3, 039906 (2015)] doi:10.1103/PhysRevD.88.055025 [arXiv:1306.4710 [hep-ph]].
- [25] E. Aprile *et al.* [XENON100], "The XENON100 Dark Matter Experiment", *Astropart. Phys.* **35**, 573-590 (2012) doi:10.1016/j.astropartphys.2012.01.003 [arXiv:1107.2155 [astro-ph.IM]].
- [26] C. E. Yaguna, "The Singlet Scalar as FIMP Dark Matter", *JHEP* **08**, 060 (2011) doi:10.1007/JHEP08(2011)060 [arXiv:1105.1654 [hep-ph]].
- [27] T. Bringmann, S. Heeba, F. Kahlhoefer and K. Vangsnes, "Freezing-in a hot bath: resonances, medium effects and phase transitions", *JHEP* **02**, 110 (2022) doi:10.1007/JHEP02(2022)110 [arXiv:2111.14871 [hep-ph]].

## A List of abbreviations

DM ... Dark matter  
SM ... Standard model  
FRW ... Friedmann-Robertson-Walker  
SU(2) ... Special unitary doublet  
GUT ... Grand Unification Theory  
SUSY ... Supersymmetry  
LSP ... Lightest supersymmetric particle  
LHC ... Large Hadron Collider  
GCE ... Grand Canonical Ensemble  
CMB ... Cosmic microwave background  
CP ... Charge and Parity  
VEV ... Vacuum expectation value  
NFW ... Navarro-Frenk-White  
TPC ... Time projection chambers

## B Programming in DarkSUSY

We describe shortly the main steps in our programming in DarkSUSY, to get the different properties we use in our plots. When modifying example programs of DarkSUSY, we always copy the files to a new folder, such that we keep the original files as well. We include pictures of the modified code where the programs was significantly modified.

### Figure 3, 4, 5 and 7

In the folders DarkSUSY → examples, we find the dsmain\_wimp.f file and its corresponding makefile. After copying these files to a new folder, we modify both the dsmain\_wimp.f and the corresponding makefile.

Modifications of the dsmain\_wimp.f:

- Deleted all the unnecessary modules in the file, kept the “model setup”, the “relic density + kinetic decoupling”, the lines 624 – 639, plus the subroutine “generic wimp”.
- Defined a new integer j
- Made a loop of the WIMP mass, by the use of integer j
- Modified the file by setting in specific values for the WIMP properties in the generic\_wimp subroutine, as shown below:

```
97 c We specify model parameters for a generic WIMP:
98 c We enter wether the WIMP is its own antiparticle or not. If WIMP=antiWIMP [0 no, 1 yes]:
99   genselfconj=1
100
101 c We enter annihilation cross section (cm^3/s):
102   gensvann=2.0d-26
103
104 c We enter PDG code for dominant annihilation channel
105 c 24 for W+W~, etc. In this case, PDG code corresponds to neutrino annihilation channel
106   genpdg=12
107
108 c We enter WIMP-nucleon scattering cross section (pb)
109   genSI=1
110
111
112   open(unit=77,file='neutrino226.dat') !We open the file we want our results in
113
114 c We create a loop over the WIMP mass
115   do j=-100,400
116     genwimp=10.0d0**(0.01*j)
117     call dsgivenodel_generic_wimp(genwimp,genselfconj,
118   &     gensvann,genpdg,genSI) !We call the model we are going to use
119     oh2=dsrdomega(0,1,xf,ierr,iwar,nfc) !We call the model we are going to use
120     write(77,*) dsmWIMP(), xf, oh2 !We specify what we want to write in our results-file.
121   enddo !In this case, WIMP mass, freeze out x and relic abundance.
122
123   close(77) !We close the file with the results
124
```

Modifications of the makefile:

- Change the DS\_MODULE to generic\_wimp in line 46
- Copy and paste lines 46-57, and insert new name for the file: my\_xf3.f instead of dsmain\_wimp.f. This is done to get the makefile to work on our modified file,



named my\_xf3.f

When running the dsmain\_wimp program in DarkSUSY, we get a file with the properties of relic abundance corresponding to varied WIMP mass, for the different averaged cross sections we choose. We also get the freeze out  $x$  of the different  $\langle\sigma v\rangle$ . Then we program the plots in Python. Fig. 3, 4 and 5 plots the different relic abundance corresponding to DM mass for different  $\langle\sigma v\rangle$ , while we plot the freeze out corresponding to mass for different  $\langle\sigma v\rangle$  in Fig. 7.

## Figure 6

In the folders DarkSUSY  $\rightarrow$  examples  $\rightarrow$  aux, we find the file oh2\_generic\_wimp.f, and the corresponding makefile. We modify the oh2\_generic\_wimp.f slightly and use the original corresponding makefile.

Modifications of the oh2\_generic\_wimp.f:

- We update the observed value of relic abundance of cold dark matter, to the newest properties from Planck 2018.
- We change one of the annihilation channels to the neutrino annihilation channel,  $PDG = 12$ .
- Rename the file that should be created with the results.

When running the oh2\_generic\_wimp program in the terminal, we get a file with the averaged annihilation cross section corresponding to the WIMP mass. We get the results for four different annihilation channels. We plot the figure in Python.

## Figure 10

In the folders DarkSUSY  $\rightarrow$  src  $\rightarrow$  rd, we find the programs dsrdeqn.f, dsmain\_wimp.f and the corresponding makefile. We modify the dsrdeqn.f, use the original dsmain\_wimp.f and modify the corresponding makefile slightly.

Modifications of the dsrdeqn.f:

- We open a file within the program, to get the program to write the results in this file.

```
70
47      open(unit=78,file='yield127.dat') !Open file we want the results in.
48
90      write(78,*) x, y, ye !Write the calculated properties we want listed in the file.
91      ! In this case x, yield, and equilibrium yield.

105
106      close (78) !Close the file with the wanted results.
107
```

Modifications of the makefile:

- Change the DS\_MODULE to generic\_wimp
- Insert the name of the folder that includes the dsrdeqn.f file, such that the makefile can run this program as well.

When running the dsmain\_wimp program of DarkSUSY in the terminal, we insert the wanted properties of the WIMP. Since we have made the makefile consider the modified dsrdeqn.f file, the program give us the values for freeze out  $x$ , yield and equilibrium yield. We run the program for three different  $\langle\sigma v\rangle$ . We then plot the figure in Python.

### Figure 13

In the folder DarkSUSY  $\rightarrow$  examples  $\rightarrow$  aux, we find the files oh2\_ScalarSinglet.f, and the corresponding makefile. We modify the oh2\_ScalarSinglet.f slightly, and use the original corresponding makefile.

Modifications of the oh2\_ScalarSinglet.f:

- Changing the observed value of relic abundance of cold dark matter to the updated value from Planck 2018.
- Writing which properties we want in the file with the results,  $x_{fo}$ ,  $m_S$  and  $\lambda$ .

When running the oh2\_ScalarSinglet program, we get the values for different scalar singlet mass,  $m_S$ , with corresponding  $\lambda$  and freeze out  $x$ ,  $x_{fo}$ . We plot the  $\lambda$  for corresponding scalar singlet mass in Python.

### Figure 14

In the folder DarkSUSY  $\rightarrow$  examples  $\rightarrow$  aux, we find ScalarSinglet\_thermal\_averages.f and its makefile. We modify the ScalarSinglet\_thermal\_averages.f, and use its original makefile.

Modifications on ScalarSinglet\_thermal\_averages.f:

- Want to use the properties of singlet scalar mass, lambda and freeze out  $x$  we found from the program to make Fig. 13. So, we open the file we created in that case, and read the values.

```
38 c... fix output file name
39   outfile = 'data/ScalarSinglet_thermal_averages.dat' !The file we want to get our results in.
40   infile = 'data/ScalarSinglet_RD_acc.dat' !The file we want to read the scalar singlet mass, lambda, and freeze out x from.
41
42
43
44
45
46   go
47   open(unit=10,file=infile) !Open the file we want to be read
48   read(10,*) inputmass, inputlambda !Read the file, and denote the columns in the file with the names inputmass and inputlambda
49
```

- We then open the file we want the new results in, and write the properties there.

```
77  open (unit=20,file=outfile) !Open the file we want the results to be in.
78  write(20,*) inputmass, dsrdthav(xf,dсанwx)*gev2cm3s, inputlambda, xf !Write the results we want in the file we opened.
79                                     !The scalar singlet mass, averaged cross section, lambda and the freeze out x
80
-----
91 500 close(20)
92  close(10) !Close both the files we have opened.
---
```

When we run this program we get  $\langle\sigma v\rangle$  from the corresponding  $\lambda$  and freeze out  $x$ , and we plot  $\langle\sigma v\rangle$  with the corresponding mass in Python.

### Figure 18

In the folders DarkSUSY  $\rightarrow$  examples  $\rightarrow$  aux, we find the files FreezeIn\_ScalarSinglet.f and its makefile. We modify FreezeIn\_ScalarSinglet.f slightly, and use the original makefile.

Modifications of FreezeIn\_ScalarSinglet.f:

- We update the value for the observed relic abundance from Planck 2018.

When we run this program we get the scalar singlet mass and corresponding  $\lambda$  in the case of the freeze in. We plot our figure in Python.